

Review

## Polysilane Dendrimers

Clemens Krempner

Department of Chemistry & Biochemistry, Texas Tech University, Memorial Dr. & Boston, Lubbock, TX 79409, USA; E-Mail: clemens.krempner@ttu.edu; Tel.: +1-806-742-3064; Fax: +1-806-742-1289

Received: 15 December 2011; in revised form: 21 January 2012 / Accepted: 29 January 2012 /

Published: 9 February 2012

---

**Abstract:** The synthesis, structure and electronic properties of polysilane dendrimers, a relatively new class of highly branched and silicon-rich molecular architectures is reviewed. After a detailed discussion of main synthetic strategies to well-defined single-core and double-core polysilane dendrimers, important structural and conformational features determined by single crystal X-ray crystallography and  $^{29}\text{Si}$ -NMR spectroscopy are presented. The last part highlights the most interesting photochemical properties of polysilane dendrimers such as UV absorption and emission behavior, which are compared with those of linear and branched polysilanes.

**Keywords:** polysilane; dendrimer; oligosilane;  $^{29}\text{Si}$ -NMR spectroscopy; UV spectroscopy; conformation; emission

---

### 1. Introduction

The last three decades have seen intense research in the field of poly- and oligosilanes, organosilicon compounds that are composed of one or more silicon-silicon bonds. Interest in this class of compounds primarily arises from their unique optical, photoelectric, and other excited state dependent properties, which result from  $\sigma$ -conjugation along the silicon main chain [1–3]. Despite their promising photo-physical properties, commercial applications have been limited by the chemical and photochemical sensitivity of the silicon-silicon bond in oligo- and polysilanes. To overcome this problem, architectures alternative to linear and cyclic polysilanes such as branched and hyperbranched polysilanes [4–7], network polysilanes (polysilyne) [8–13] ladder polysilanes [14], organosilicon nanoclusters [15–17] and also dendritic polysilanes have been proposed and investigated [18–50].

The chemistry of well-defined polysilane dendrimers dates back to 1995, when Lambert *et al.* [18] and Suzuki *et al.* [19] independently reported the synthesis and structure of the first polysilane

dendrimer of first generation,  $\text{MeSi}[\text{SiMe}_2\text{Si}(\text{SiMe}_3)_3]_3$ . Soon after the synthesis and structural characterization of further dendritic polysilanes including the first polysilane dendrimer of second generation reported by Sekiguchi *et al.* [20], the field developed rapidly, in part driven by the belief that polysilane dendrimers have the potential of being useful as optoelectronic materials. In fact, polysilane dendrimers combine photo-physical properties with good solubility—similar to linear polysilanes—but have higher thermal and chemical resistance. Moreover, the well-defined molecular nature of polysilane dendrimers allowed for detailed structural studies using single crystal X-ray crystallography and various spectroscopic techniques. Although the chemistry of polysilane dendrimers is still in its early stage, certain aspects of this chemistry have already been covered in two short reviews [30,35] and a book chapter [49]. This more comprehensive review seeks to thoroughly cover the entire field of polysilane dendrimers. Special emphasis is given to the synthesis, solid-state structures,  $^{29}\text{Si}$ -NMR spectroscopy and electronic properties. The structural and electronic properties of polysilane dendrimers will be compared with those of simple branched and linear polysilanes.

## 2. General Remarks

There are two subgroups of dendritic polysilanes, single-core dendrimers (S) and double-core dendrimers (D) (Figures 1 and 2). Both types of dendrimers display four main structural characteristics. (1) The core silicon atom (c) in all known single-cored structures is bound exclusively to three silicon atoms that begin the dendrimer wings (W). Dendrimers that have a central silicon core bound to four silicon atoms have not been reported so far, presumably due to repulsive steric interactions between the dendrimer wings, which render the formation of such highly strained compounds thermodynamically unfavourable [46]. In double-cored structures, the core silicon atom is connected to two silicon atoms that begin the dendrimer wings (the silicon spacer group that connects the two cores is not included!). Again, due to repulsive interactions, stable double-cored dendrimers with cores that have three wings have not been observed so far. Following Lambert's [35] suggestions we assign the designation  $c = 2$  when two wings are bound to the core (didendrons) and  $c = 3$  for three wings bound to the core (tridendrons); (2) In both single- and double- core structures the core silicon (c) may have any number of silicon atom spacers between the core and the first branch point. The number of silicon spacer atoms is defined by  $s$ ;  $s = 0$  (no spacer atom);  $s = 1$  (one spacer atom) and so on. In double-core structures the spacer silicon chain that connects the two silicon cores (c) may have any number of silicon atoms. When there are no silicon spacer atoms,  $n = 0$ ; when there is one spacer atom,  $n = 1$ , when there are two spacer atoms,  $n = 2$  and so on; (3) The silicon atom ( $\text{Si}^*$ ), which represents the branch point may have either two ( $-\text{Si}^*\text{Si}_2$ ) or three ( $-\text{Si}^*\text{Si}_3$ ) additional silicon atoms that emanate from it. The number of those silicon atoms is defined as (b);  $b = 2$  for two-fold branching and  $b = 3$  for three-fold branching; (4) The generation of the dendrimer is defined as (g). If there is only one branch point on each dendrimer wing we assign the designation  $g = 1$  for first generation dendrimers. If a second branch point follows, the molecule is designated  $g = 2$  for a second generation dendrimer. Thus, for single-core polysilane dendrimers the designation  $S\text{-}gcsb$  is used, whereas double-core dendrimers are referred to as  $D\text{-}gcsb\text{-}n$ .

Figure 1 shows the single-core dendrimers **1-3** of first generation with either no ( $s = 0$ ) or one ( $s = 1$ ) spacer silicon atom between the core and the branch point. To reach a valency of four, typical for silicon, either exclusively methyl groups (referred to as permethylated dendrimers) or methyl groups along with some functional groups (halides, OH, metals, phenyls) are attached to each silicon atom. Because in both dendrimers **1** and **2** the core silicon is three-fold and the branch silicons are two-fold, the structures are referred to as **S-1302** and **S-1312**. Dendrimer **3** on the other hand is designated as **S-1313** because both core silicon and branch silicons are three-fold and the number of spacer silicon atoms is one.

**Figure 1.** Single-core dendrimers of first generation (all non-silyl groups are omitted for clarity, blue = branch point, brown = spacer, red = core).

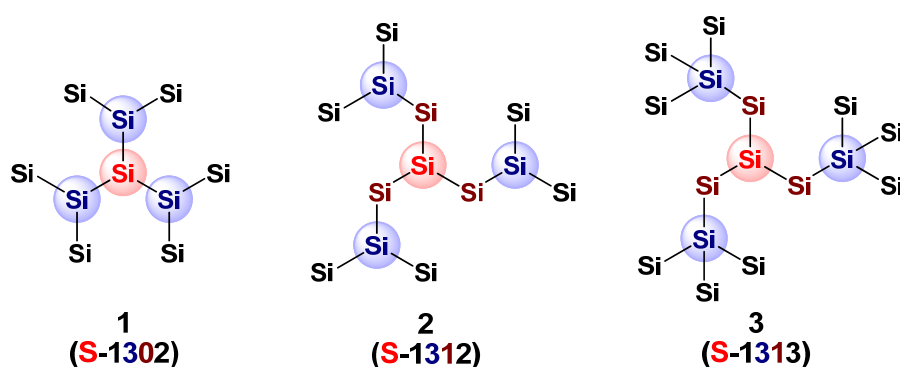
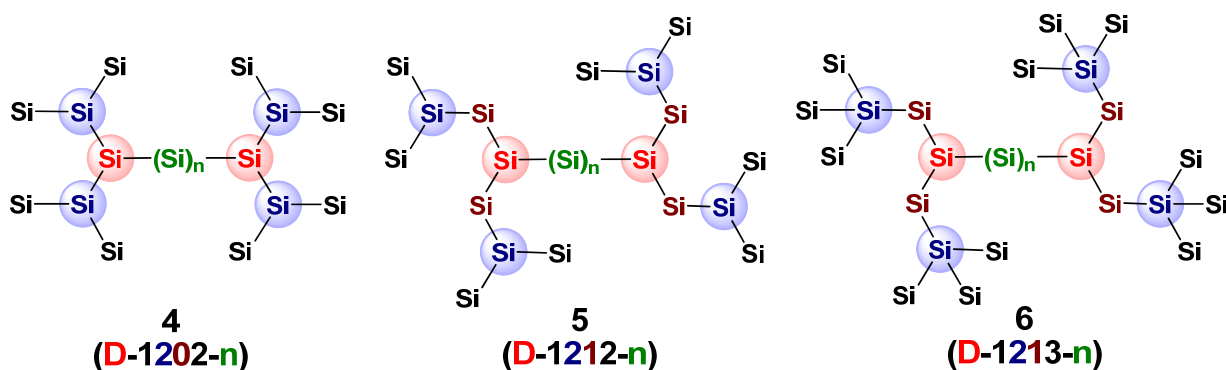


Figure 2 contains double-core dendrimers of first generation with either zero or one spacer silicon atom between the core and the branch point ( $s = 0, 1$ ). These dendrimers, however, may or may not have an additional silicon spacer group located between the two cores, a structural feature that is distinct from single-core dendrimers. Accordingly, we assign the designation  $n = 0$  for no spacer silicon atom between cores,  $n = 1$  for one silicon atom between cores, and so on. The structures **4** and **5** are referred to as **D-1202-n** and **D-1212-n**, because in both cases the core is two-fold and the branch points are two-fold and the number of silicon spacer atoms between the cores is equal to  $n$ . Dendrimer **6** is designated **D-1213-n** since the branch points are threefold and the number of spacer silicon atoms between core and branch is one.

**Figure 2.** Double-core dendrimers of first generation (all non-silyl groups are omitted for clarity; blue = branch point, brown = spacer, red = core, green = spacer between cores).



### 3. Synthetic Strategies

The key step in the synthesis of well-defined polysilane dendrimers is the selective formation of silicon-silicon bonds through either Wurtz-type coupling, salt metathesis or a combination of both methods. In a Wurtz-type coupling reaction silicon halides or triflates are coupled reductively by using group 1 metals to form silicon-silicon bonds with elimination of metal salt. This method is particularly useful for the preparation of permethylated branched oligosilanes such as  $\text{Si}(\text{SiMe}_3)_4$  and  $\text{MeSi}(\text{SiMe}_3)_3$  first reported by Gilman and coworkers [51–53]. These branched structures are important precursors for the generation of cores, wings and dendrons. In salt metathesis chemistry suitable silicon nucleophiles, also referred to as silyl anions or metal silanides (for reviews see also [54–58]), are treated with silicon electrophiles such as organosilicon chlorides, bromides or triflates to selectively form Si-Si bonds, again with the elimination of metal salt. This type of silicon-silicon bond formation reaction usually proceeds with higher selectivity and therefore is more suitable for the connection of cores with wings to generate dendritic structures of first and second generation.

#### 3.1. Cores, Spacers and Wings

The synthesis of the branched oligosilanes **7–11**, precursor compounds for the construction of core structures and wings, is shown in Figure 3. Reductive coupling of mixtures of  $\text{SiCl}_4$  and  $\text{Me}_3\text{SiCl}$  with elemental lithium in THF (Tetrahydrofuran) gives access to **7** in yields of 60–80% [59]. Reductive coupling of mixtures of  $\text{MeSiCl}_3$  and  $\text{Me}_3\text{SiCl}$  with elemental lithium in THF produces **10** as the major product in *ca.* 60–75% yields and **11** as the byproduct in *ca.* 20–25% yield [60]. The phenyl functionalized silanes **8** and **9** were synthesized in yields of *ca.* 70% by treatment of  $\text{LiSiMe}_2\text{Ph}$  with  $\text{PhSiCl}_3$  and  $\text{MeSiCl}_3$ , respectively [32,61]. All five oligosilanes are air- and moisture-stable compounds that can be prepared on a *ca.* 50 g scale and purified easily by vacuum distillation or sublimation.

The introduction of multiple functional leaving groups can be achieved by selective chlorodemethylation of **7**, **10** and **11** [62–66] and by chlorodephenylation of **8** [67]. Both types of reactions proceed with high selectivities to furnish the chlorosilanes **12**, **13**, **15** and **16** each in excellent yields as moisture-sensitive but air-stable compounds. Again, purification of these compounds can be carried out easily by vacuum distillation or sublimation. The triflate-functionalized core structure **14** can conveniently be generated via protodesilylation of **9** with three equivalents of trifluoromethanesulfonic acid [20]. The hexachloro-functionalized silane **17** is generated by base-induced redistribution of  $\text{Cl}_2\text{MeSi-SiMeCl}_2$  (derived from chlorination of the Mueller-Rochow disilane fraction) [68,69].

Wing structures that contain silyl anions (herein referred to as metalated wings) can conveniently be generated from oligosilanes **7**, **9** and **10** by a synthetic approach that was first developed by the groups of Gilman and Brook and involves selective cleavage of silicon-silicon bonds by strong metallo-nucleophiles. For example, reaction of  $\text{LiMe}$  with **7** and **10**, respectively, generates after 2–3 days the highly air- and moisture-sensitive branched lithium silanides  $\text{Li-18}$  [70,71] and  $\text{Li-19}$  [72] (Figure 4). Similarly, branched polysilane **21** [73] can be converted into  $\text{Li-22}$  [74] in good yields (Figure 5). Recently, Marschner developed an easy and cheap synthetic method that gives access to a

wide variety of potassium silanides via the selective cleavage of a Si-Si bond with  $\text{KOBU}^\dagger$  in THF [75]. Using this straightforward synthetic protocol, the potassium silanides **K-18** [75], **K-19** [76] and **K-20** [41] (Figure 4) and also **K-22** [77] (Figure 5) could be generated within a few hours in almost quantitative yields. Both, lithium and potassium silanide wings are used as strong nucleophiles in the selective formation of Si-Si bond required for the assembly of the final polysilane dendrimer. The use of the more reactive potassium silanides, however, allows for the isolation of the raw dendrimer in higher purities and yields and facilitates the purification of the dendrimer.

**Figure 3.** Synthesis of single-core and double-core units that contain multiple leaving groups (red = core, blue = leaving group for nucleophilic substitution reactions).

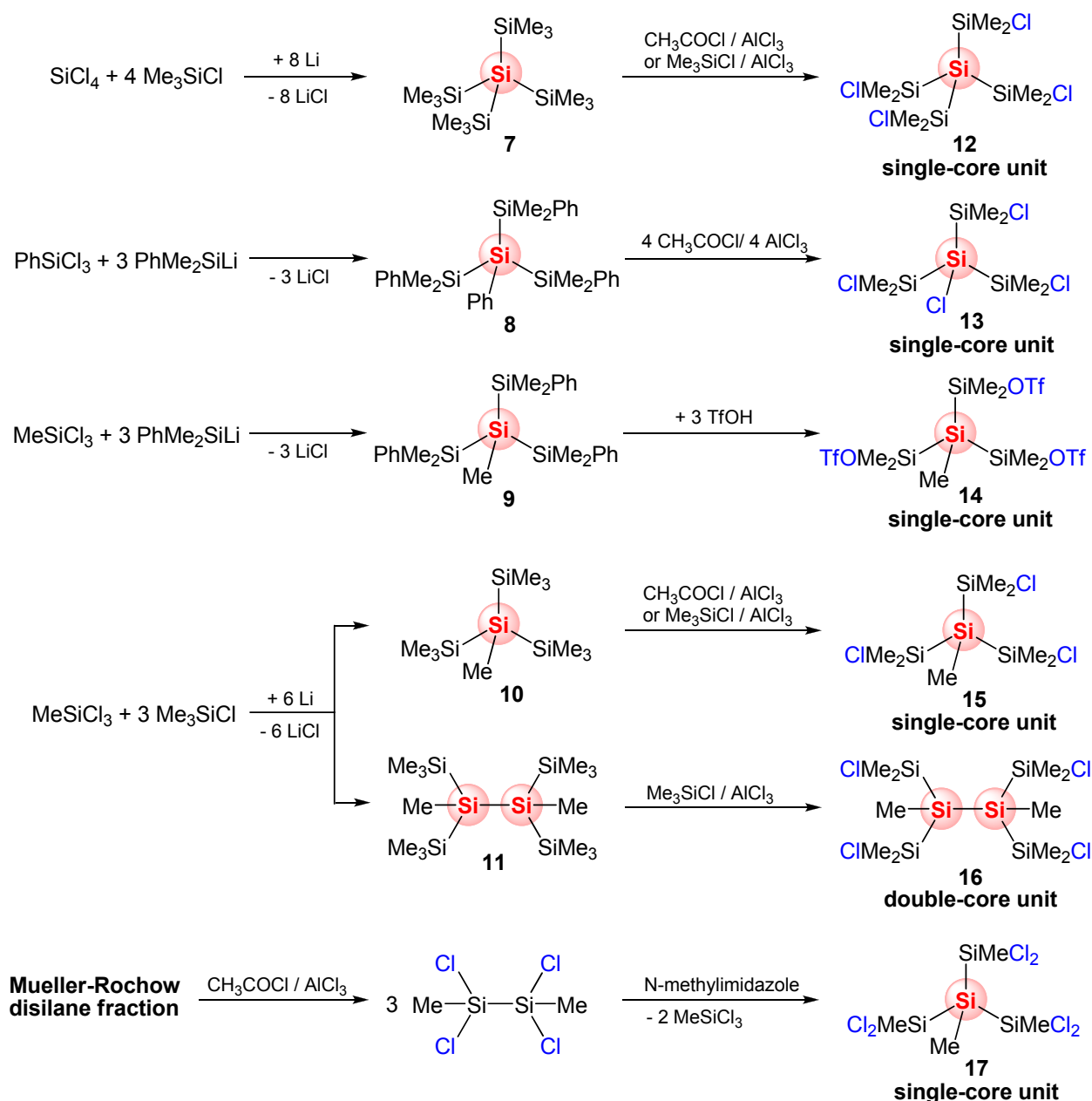


**Figure 4.** Formation of the metalated wings M-18, M-19 and M-20 (M = Li, K; dark-blue = branch point, blue = chemically active group).

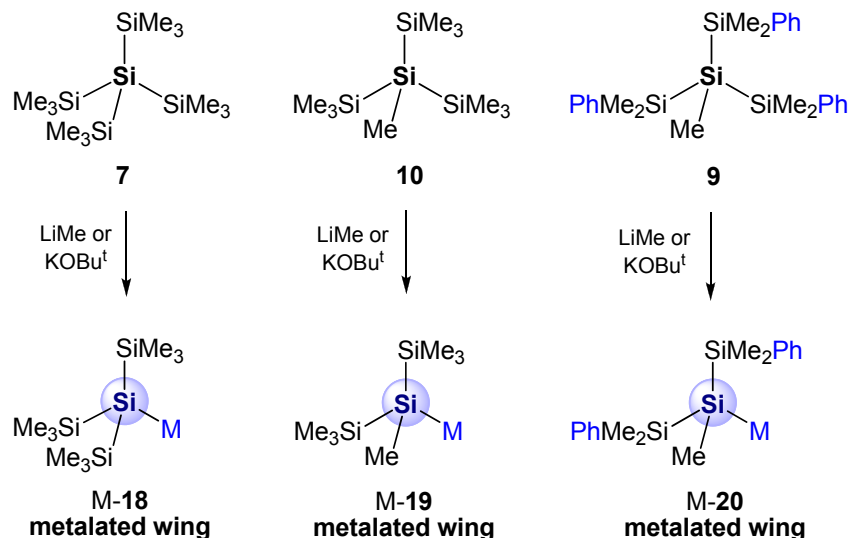
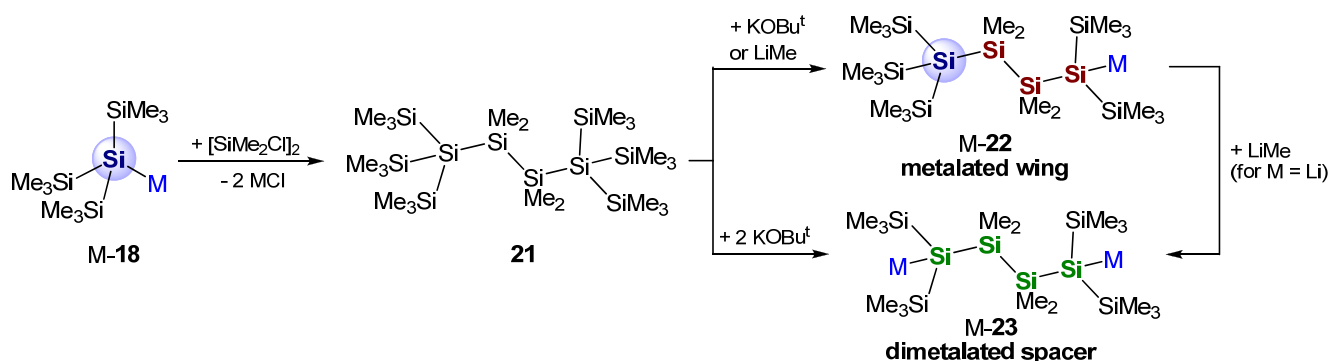


**Figure 5.** Synthesis of branched oligosilanes and metal silanides (wings) [brown = spacer silicon, dark blue = branch point, blue = chemically active group].



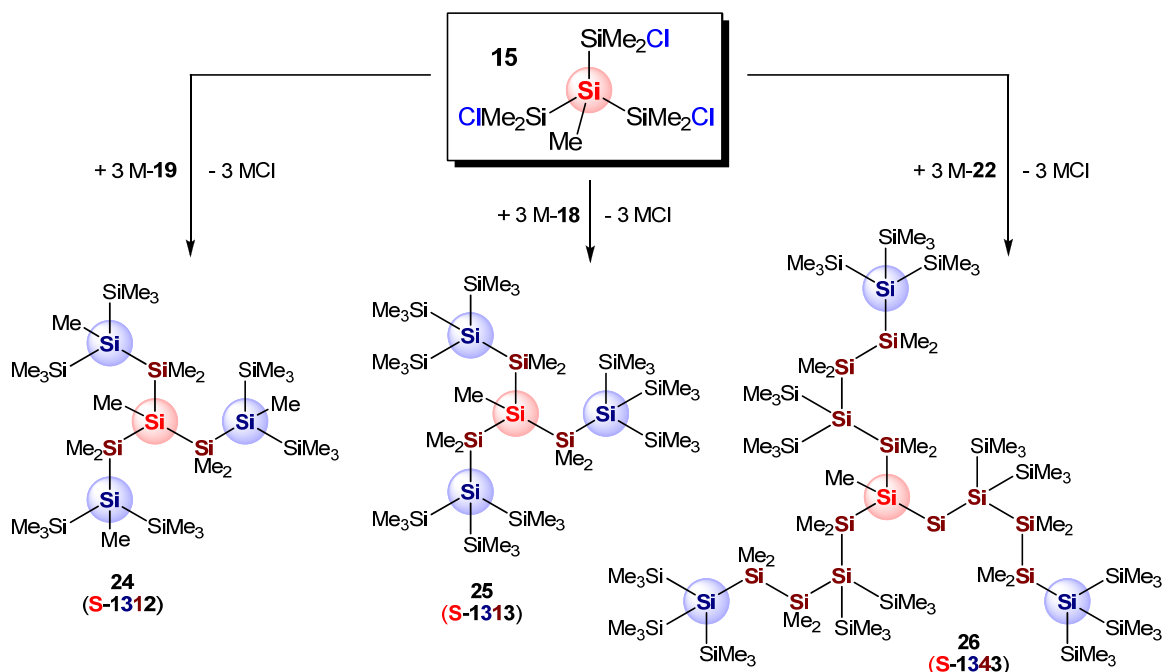
An extension of this synthetic approach to oligosilanes that contain two Si-M functionalities is shown in Figure 5. Reaction of two equivalents of  $\text{KOBu}^t$  with branched oligosilane **21** in THF at elevated temperatures gave access to the dipotassium disilanide **K-23** in excellent yields [77]. Dilithiated disilanide **Li-23** was obtained in modest overall yields in two steps [74]. Compound **K-23** proved to be useful as a metalated spacer unit for the construction of large double-core polysilane dendrimers of first generation via silicon-silicon bond formation chemistry.

### 3.2. Regular Single-Core Polysilane Dendrimers of First Generation

In 1995 Lambert *et al.* [18,24] and Suzuki *et al.* [19] independently reported the convergent synthesis and structure of the first polysilane dendrimers of first generation (Figure 6). Both groups used a similar synthetic approach involving reactions of the lithiated wing units **Li-18**, **Li-19** and **Li-22**, respectively, with core structure **15** which generated the regular single-core dendrimers **24** (**S-1312**), **25** (**S-1313**) and **26** (**S-1343**). These reactions proceeded rapidly with formation of three new silicon-silicon bonds via elimination of lithium chloride. Notably, dendrimer **26**, structurally

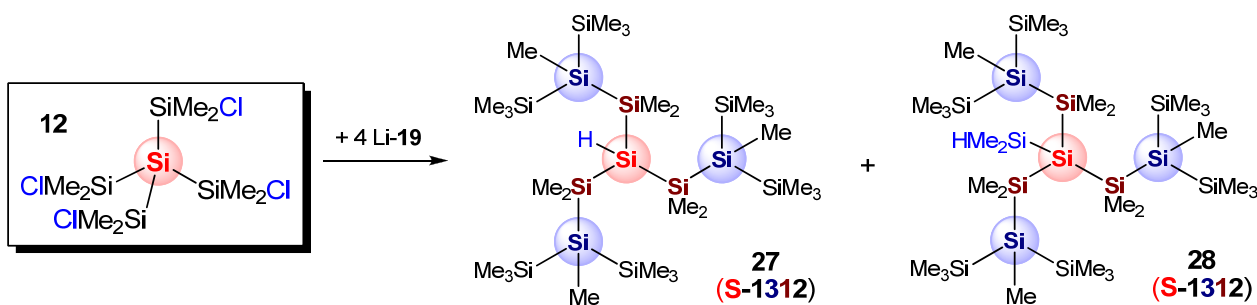
characterized by X-ray crystallography, is composed of 31 silicon atoms, has a molecular weight of 1833 and has 13 silicon atoms in the longest silicon chain. It is the largest single-core dendrimer prepared to date [24].

**Figure 6.** Convergent synthesis of regular polysilane dendrimers of first generation (red = core, brown = spacer silicon, dark blue = branch point, blue = chemically active group).



Attempts to synthesize first generation polysilane dendrimers with four wings emanating from the central core failed, primarily for steric reasons [46]. For example, treatment of core structure **12** with four equivalents of Li-19 led to partial reduction and fragmentation processes resulting in the formation of **27** and **28** as low-yield byproducts (Figure 7) [21,27]. Both molecules, however, represent further examples of regular polysilane dendrimers of first generation with three wings emanating from the central core. Hydrido-functionalized dendrimer **27** (S-1312) is closely related to **24** (S-1312), in which the methyl group bound to the central core is replaced by H.

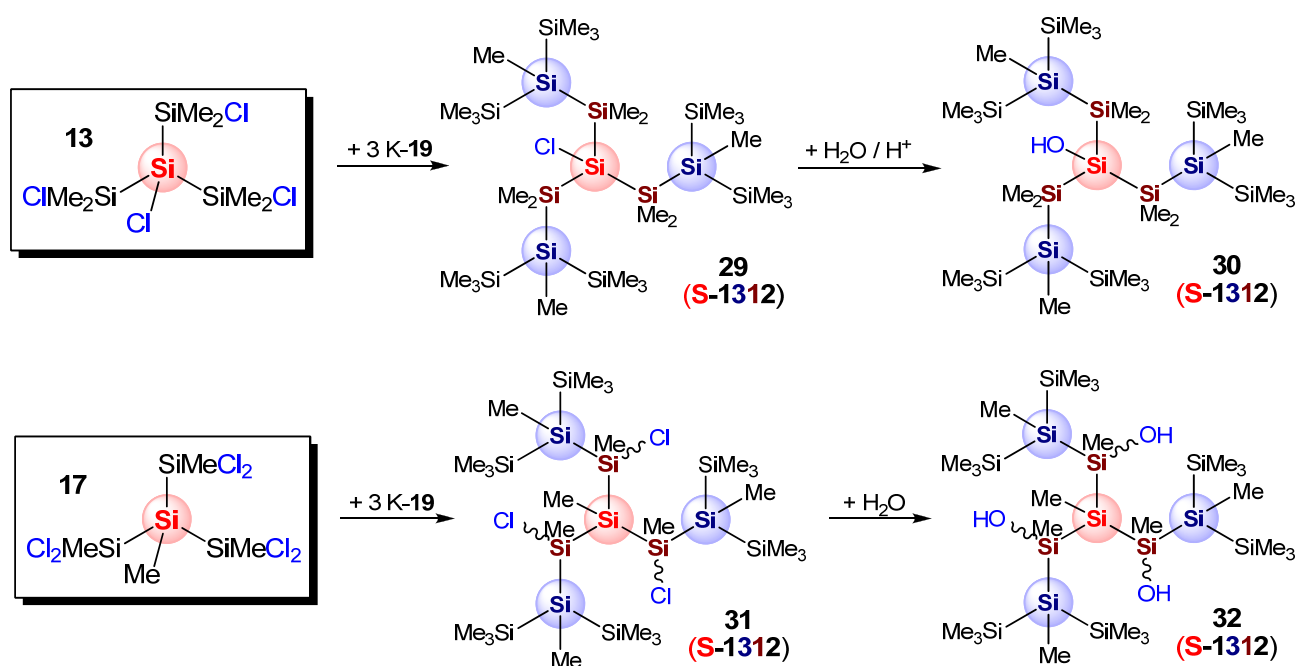
**Figure 7.** Synthesis of core-functionalized polysilane dendrimers of first generation (red = core, brown = spacer silicon, dark blue = branch point, blue = chemically active group).



Recently, Krempner *et al.* have shown that a variety of core- and spacer-functionalized single-core dendrimers of first generation can be prepared easily and in high yields by modifying the number and

position of the leaving chloro groups at the iso-tetrasilane single-core units (Figure 8). For example, reaction of potassium silanide K-19 with iso-tetrasilane **13** gave the remarkably stable chloro-functionalized dendrimer **29** [43]. Subsequent hydrolysis in the presence of sulfuric acid slowly but almost quantitatively generated the hydroxo-substituted dendrimer **30** [50]. Treatment of hexachloro substituted iso-tetrasilane **17** with potassium silanide K-19 in hexanes furnished the trichloro-substituted dendrimer **31** in excellent yields [42]. The reaction proceeds with high regio- and diastereoselectivity to form the *l,l*-form of **31** as the only detectable diastereomer. Hydrolysis of *l,l*-**31** in the presence of  $\text{NH}_4(\text{H}_2\text{NCOO})$  gave racemic mixtures of the two possible diastereomers *l,l*-**32** and *l,u*-**32** with the latter form being the major diastereomer [42]. In contrast, hydrolysis of *l,l*-**31** without base gave *l,l*-**32** as the major diastereomer [48].

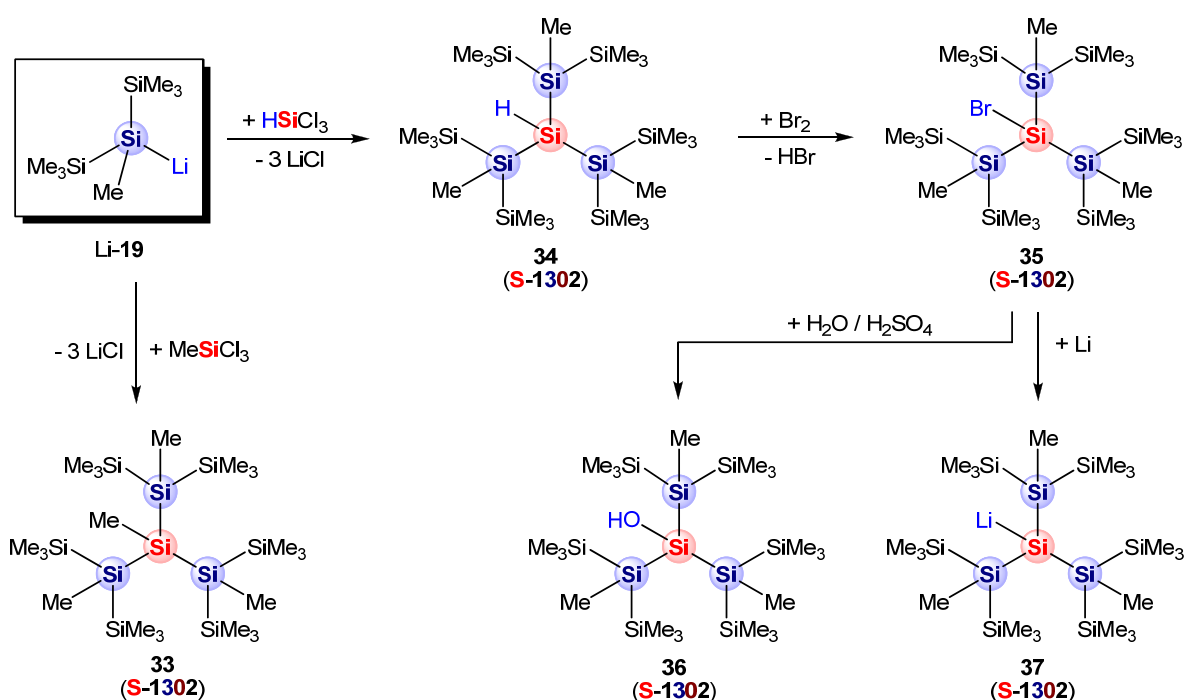
**Figure 8.** Synthesis of core- and spacer-functionalized polysilane dendrimers of first generation (red = core, brown = spacer silicon, dark blue = branch point, blue = chemically active group).



In 1996, Lambert *et al.* reported the first convergent synthesis and solid-state structure of permethylated polysilane dendrimer **33** (S-1302), the smallest dendritic polysilane with a total of 10 silicon atoms and a longest silicon chain with 5 silicon atoms [21] (Figure 9). Compound **33** was obtained in fairly low yields (16%) from the reaction of Li-19 with  $\text{MeSiCl}_3$  in THF, along with a cyclic by-product arising from silicon-silicon bond cleavage processes. Krempner *et al.* found that formation of cyclic by-products can be suppressed by replacing the solvent THF with n-pentane and by adding neat  $\text{MeSiCl}_3$  to a pentane solution of Li-19 at  $-78^\circ\text{C}$ . This synthetic protocol allowed for the preparation of **33** in much higher yields (78%). Reacting  $\text{HSiCl}_3$  with Li-19 under similar experimental conditions gave the hydrido-functionalized dendrimer **34** in yields of 67%. **34** proved to be a useful precursor for the synthesis of various other core-functionalized first-generation polysilane dendrimers (Figure 9) [31,32]. Note, however, that in these dendrimers the three emanating wings are directly connected to the central core with its functional group because of the absence of spacer groups. This

structural arrangement enforces steric repulsion between wings and core and is therefore inappropriate for the construction of stable polysilane dendrimers of higher generation. On the other hand, the functionalized core is fully encumbered by the three wings, which results in enhanced hydrolytic stabilities of, for example, dendritic bromo silane **35**. Notably, no hydrolysis of **35** in water occurred; only in the presence of sulfuric acid **35** slowly hydrolyzed to the OH-functionalized dendrimer **36**. Lithiation of dendritic bromosilane **35** led to the formation of the first metalated dendrimer **37** as an air- and moisture sensitive but thermally stable red solid; no fragmentation of the dendritic silicon backbone occurred even at higher temperature [38,39].

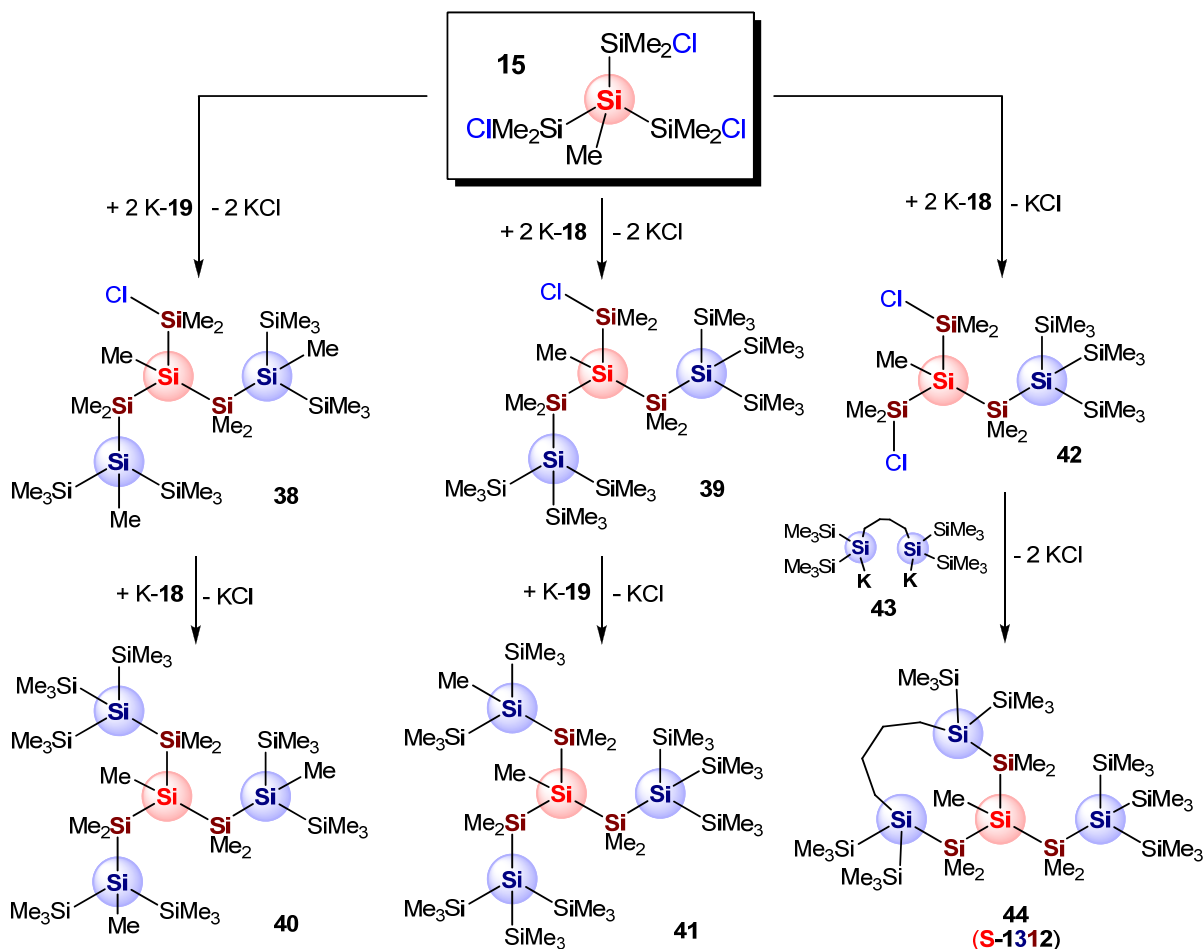
**Figure 9.** Synthesis of core-functionalized polysilane dendrimers of first generation (red = core, dark blue = branch point, blue = chemically active group).



### 3.3. Irregular Single-Core Polysilane Dendrimers of First Generation

The synthesis of irregular single-core dendritic polysilanes was motivated by efforts to compare structural and spectroscopic properties of dendrimers with the same silicon chain length, but with different substitution patterns [45]. The preparation of irregular dendrimers requires a stepwise assembly of strategic silicon-silicon bonds using differently structured metalated wings to be attached to the central core unit. As shown in Figure 10, reactions of two equivalents of either **K-19** or **K-18** with **15** lead to the formation of the chloro-functionalized polysilane dendrons **38** and **39**, respectively. Subsequent treatment of **38** with **K-18** and **39** with **K-19** furnished the irregular single-core polysilane dendrimers **40** and **41**, respectively. On the other hand, reaction of the dichloro silane **42** (derived from the stoichiometric reaction of **15** with **K-18**) with dipotassium disilanide **43** [78] gave the first carbocyclic polysilane dendrimer **44** in modest yields.

**Figure 10.** Synthesis of irregular polysilane dendrimers of first generation (red = core, brown = spacer silicon, dark blue = branch point, blue = chemically active group).



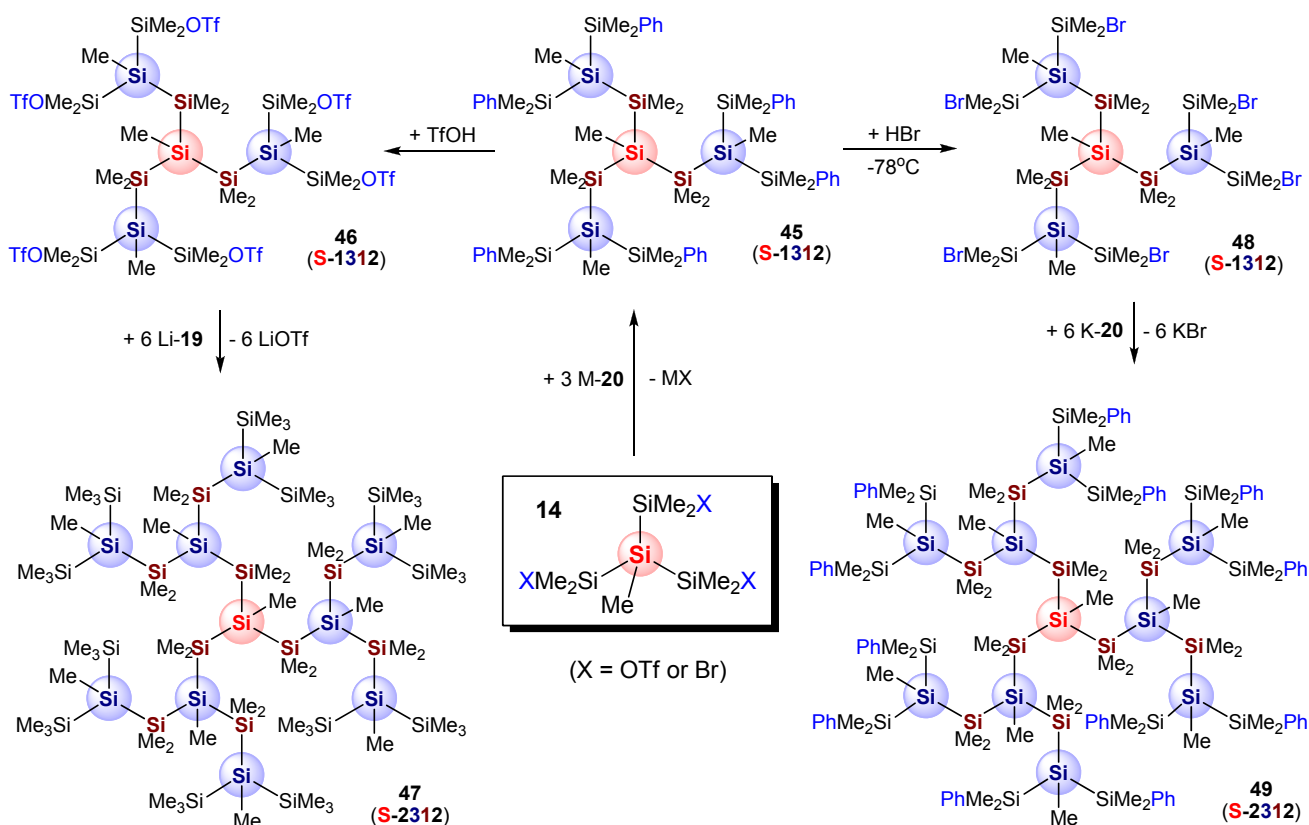
### 3.4. Single-Core Polysilane Dendrimers of Second Generation

Sekiguchi's group was the first to report the synthesis of a single-core polysilane dendrimer of second generation **47** by using a divergent synthetic methodology (Figure 11) [20]. In the first step, silyl triflate **14** ( $X = \text{OTf}$ ) was generated *in situ* from the reaction of TfOH with **9** (see also Figure 4) and subsequently reacted with 3 equivalents of lithium silanide Li-**20** to afford the phenyl-functionalized first-generation dendrimer **45** (**S-1312**) in 43% yield. Finally, dendrimer **47** was obtained in yields of 29% by dephenylation of **45** with TfOH, followed by addition of Li-**19**. Later, Sekiguchi *et al.* [28] and Marschner *et al.* [41] reported an improved procedure for the synthesis of phenylated dendrimer **45**. Replacement of silyl triflate **14** ( $X = \text{OTf}$ ) with either bromosilane **14** ( $X = \text{Br}$ ) or chlorosilane **15** avoided frequently encountered side-reactions of strong nucleophiles such as metal silanides with silyl triflates and produced **45** in much better yields (74% in both cases).

Marschner *et al.* also reported the synthesis of **49**, a phenyl-substituted regular polysilane dendrimer of second generation, in good overall yields (Figure 11) [41]. Dendrimer **45**, derived from the reaction of bromosilane **14** ( $X = \text{Br}$ ) with potassium silanide K-**20**, was treated with neat HBr at  $-78^\circ\text{C}$  to furnish the bromo-substituted first generation dendrimer **48** in 83% yield. Subsequent reaction **48** with K-**20** gave access to dendrimer **49** in yields of 41%. Notably, compounds **47** and **49** are the only examples of a regular polysilane dendrimers of second generation; both are composed of 31 silicon

atoms and have longest chains of 13 silicon atoms. The structure of **47** was unambiguously identified by single-crystal X-ray crystallography (Figure 15) [20].

**Figure 11.** Synthesis of single-core polysilane dendrimers of second generation (red = core, brown = spacer silicon, dark blue = branch point, blue = chemically active group).

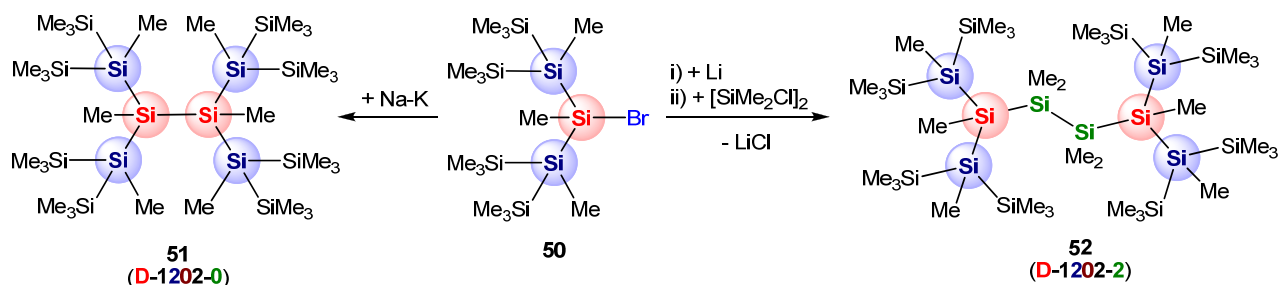


### 3.5. Double-Core Polysilane Dendrimers of First Generation

The synthesis and solid-state structure of dendritic silane **51** (Figure 12), the first double-core polysilane dendrimer was reported by Lambert *et al.* in 1998 [24]. Later, Krempner *et al.* published an improved synthesis via reductive coupling of bromo-functionalized dendron **50** with Na-K alloy, which gave **51** in yields of 32% [40]. Dendrimer **51** is of first generation with a longest chain of 6 silicon atoms and a total of 14 silicon atoms. Again, because of the absence of any silicon containing spacer groups the cores of the two dendrons are directly connected with each other, which introduces significant steric strain in the molecule. These repulsive steric interactions render the construction of double-core polysilane dendrimers of higher generation impossible.

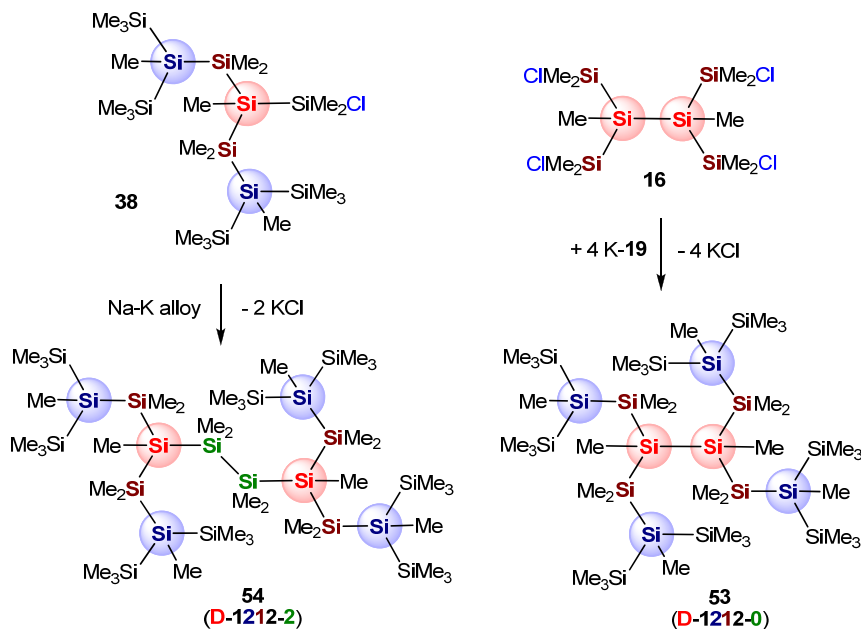
Shortly after, Krempner *et al.* synthesized a variety of new double-core polysilane dendrimers of first generation and showed by means of X-crystallography that introducing spacer silicon groups in various positions indeed reduces the steric strain significantly [37]. For example, dendrimer **52** (Figure 12), derived from lithiation of **50** and subsequent addition of ClMe<sub>2</sub>SiSiMe<sub>2</sub>Cl, contains two silicon spacer groups between both central cores, which minimizes steric interactions between the two dendrons.

**Figure 12.** Synthesis of double-core polysilane dendrimers of first generation (red = core, dark blue = branch point, green = spacer silicon atoms between the cores, blue = chemically active group).



Spacer silicon groups were also incorporated between core and branch point such as in dendrimer **53**, which was prepared by treatment of 4 equivalents of potassium silanide K-19 with the chloro-functionalized double-core unit **16** via salt metathesis (Figure 13). Reductive coupling of dendron **38** with Na-K alloy furnished the double-core polysilanes dendrimer **54** that contains spacer silicon groups between both cores and branch point and core. Compound **54** has a longest chain of 10 silicon atoms and total of 20 silicon atoms [44].

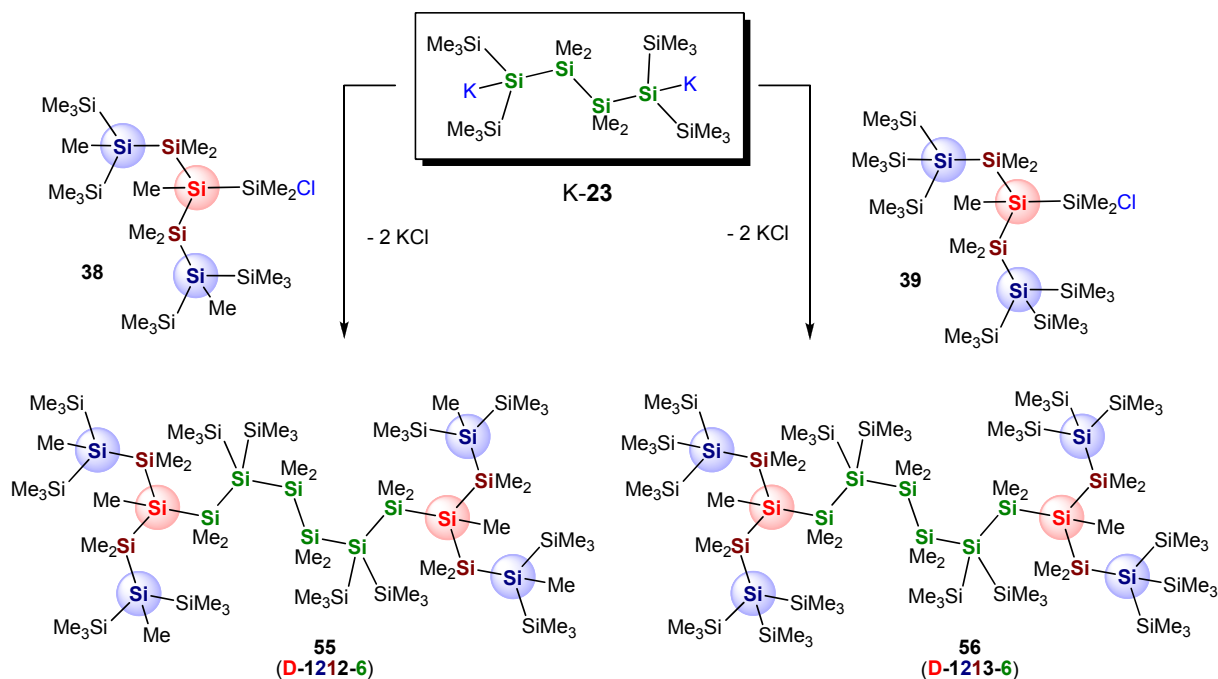
**Figure 13.** Synthesis of double-core polysilane dendrimers of first generation (red = core, brown = spacer silicon, dark blue = branch point, green = spacer silicon atoms between the cores, blue = chemically active group).



Recently, the Krempner lab reported a synthetic strategy to even larger double-core polysilane dendrimers involving a convergent methodology [47]. Key to this approach is the generation of dimetalated oligosilane K-23 published by Marschner and coworker (see also Figure 5) [77], which in reactions with the chloro-functionalized dendrons **38** and **39** afforded the double-core dendrimers **55** (D-1312-6) and **56** (D-1313-6), respectively, in good yields (Figure 14). In particular polysilane **56** is worth mentioning as it represents the largest dendritic polysilane prepared to date; it has a longest

chain of 14 silicon atoms and a total of 32 silicon atoms. Both compounds have been characterized by X-ray crystallography and NMR spectroscopy.

**Figure 14.** Synthesis of double-core polysilane dendrimers of first generation (red = core, brown = spacer silicon, dark blue = branch point, green = spacer silicon atoms between the cores, blue = chemically active group).



#### 4. X-Ray Crystallography

Since all synthesized polysilane dendrimers are well-defined crystalline materials, most (except for **41**, **54** and **49**) have been structurally unambiguously characterized by means of single-crystal X-ray crystallography. The solid-state structures of the largest polysilane dendrimers **47**, **55** and **56** (top- and side view) along with their corresponding Connolly surfaces are shown in Figures 15, 16 and 17, respectively. All three dendrimers are in the nanometer size regime even though shape and size differ considerably. The bond lengths and bond angles in the periphery of all structurally characterized polysilane dendrimers are in the expected range with Si-Si distances ranging from *ca.* 235–236 pm and Si-Si-Si angles deviating by only 3–4° from the ideal tetrahedral angle [79]. However, the inner Si-Si distances ranging from 236–240 pm and some of the inner Si-Si-Si angles ranging from 108 up to 129° are significantly larger, which indicates repulsive steric interactions in these dendrimers. Figure 18 illustrates the approximate structure of the interior silicon backbone of spacer-containing polysilane dendrimers with formally two-fold (left) and/or three-fold branch points (right). The average Si-Si distances and Si-Si-Si angles of the two types of silicon backbones are listed in Table 1. A comparison of the values implies that steric strain is most pronounced in dendrimers with exclusively three-fold branches, in which four silicon atoms are linked to the branch silicon. The increased number of substituents being in close proximity to the branch silicon enforces steric repulsion between the individual substituents, which is partially reduced by larger Si-Si distances and wider Si-Si-Si angles.

**Figure 15.** Solid-state structure of **47** with Connolly surface (side view left; top view right; ● = core silicon; ● = spacer silicon; ● = branch silicon; ● = primary silicon; ● = carbon; white = hydrogen).

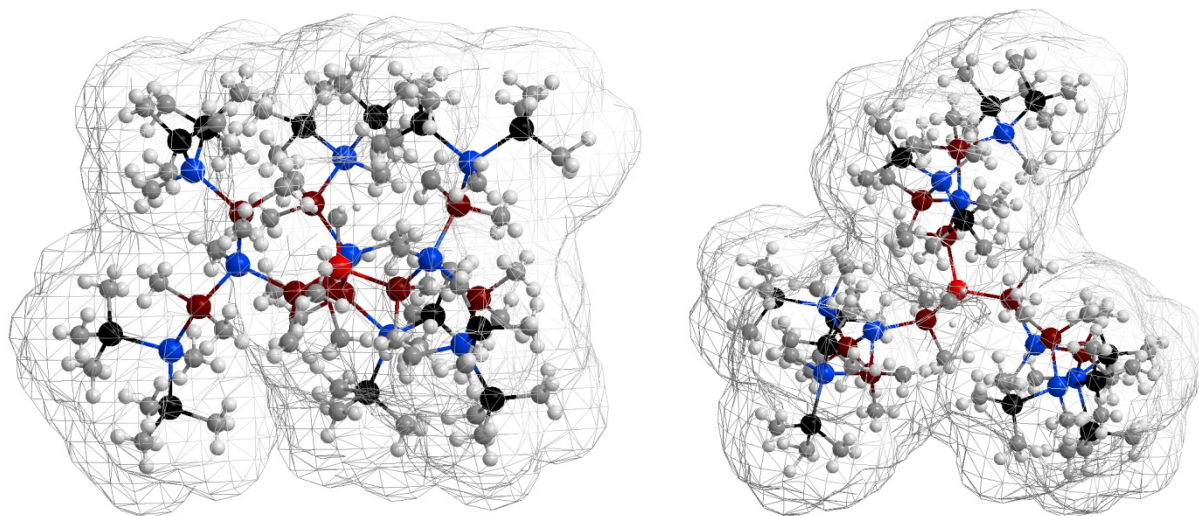


**Figure 16.** Solid-state structure of **55** with Connolly surface (side view left; top view right; ● = core silicon; ●/● = spacer silicon; ● = branch silicon; ● = primary silicon; ● = carbon; white = hydrogen).

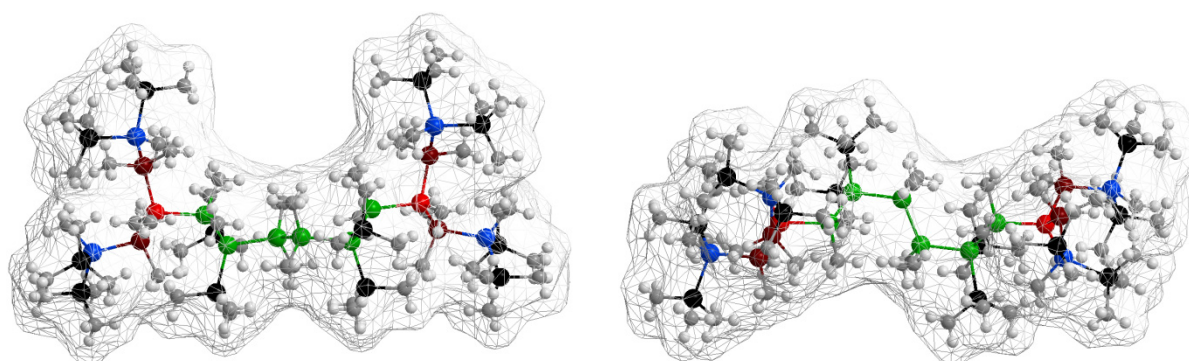


**Figure 17.** Solid-state structure of **56** with Connolly surface (side view left; top view right; ● = core silicon; ●/● = spacer silicon; ● = branch silicon; ● = primary silicon; ● = carbon; white = hydrogen).

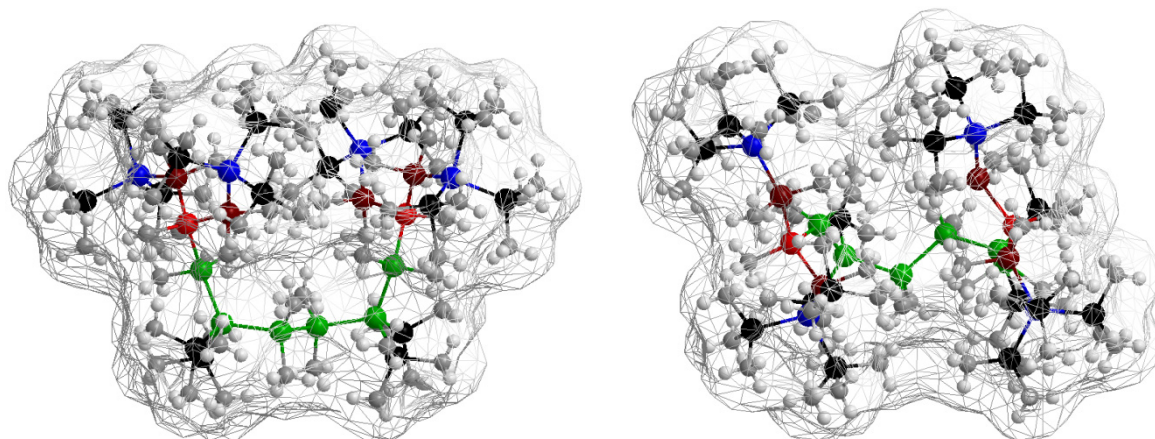


**Figure 18.** Approximate structures of the central silicon-silicon backbone of polysilane dendrimers with formally two-fold branches (**left**) and three-fold branches (**right**) (all C and H atoms and some silicon atoms in the periphery are omitted for clarity).

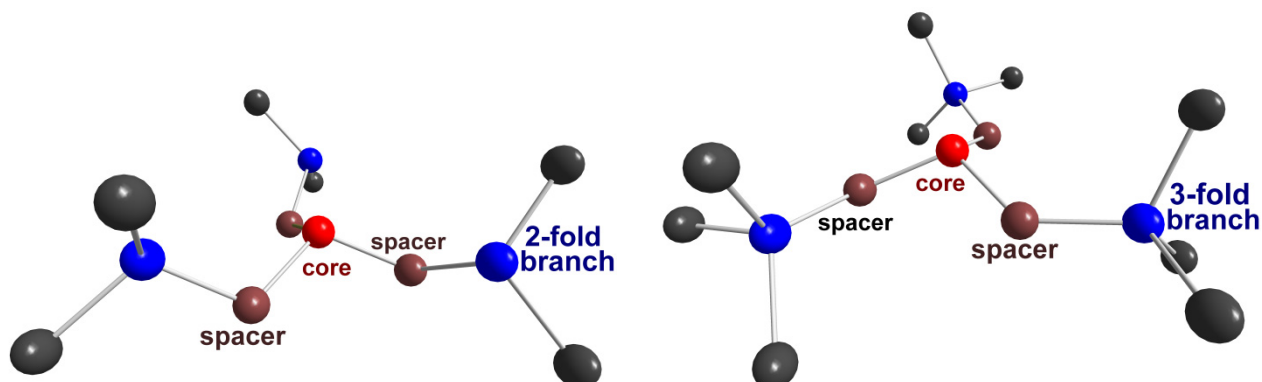


**Table 1.** Average Si-Si distances [pm] and Si-Si-Si angles [°] of selected polysilane dendrimers with 2-fold and 3-fold branch points (● = core silicon; ●/● = spacer silicon; ● = branch silicon; ● = primary silicon; all methyl groups are omitted for clarity).

No.	Structure	Branch	Si-Si-Si spacer-core- spacer	Si-Si-Si core-spacer- branch	Si-Si core- spacer	Si-Si spacer- branch	Ref.
24		2-fold	108	115	237	236	[28]
47		2-fold	109	119	239	238	[20]
55		2-fold 3-fold	107 110	116 123	238 239	237 238	[47]
40		2-fold 3-fold	106 111	116 119	239 239	238 237	[45]
53		2-fold	110	116	239	236	[44]
25		3-fold	112	129	237	240	[19]
56		3-fold	111	129	237	239	[47]
26		3-fold	111	128	238	239	[24]

For example, the average Si-Si distances (spacer-branch) for dendrimers with exclusively three-fold branches, are relatively large ranging from 239–240 pm, whereas the values of dendrimers with only two-fold branches are slightly smaller with values ranging from 236–238 pm, even though the three Si-Si bonds emanating from the central core (core-spacer) are rather similar for both types of dendrimers ranging from 237–239 pm. Most remarkable, however, are the relatively large average Si-Si-Si angles emanating from the core silicon (core-spacer-branch), which by flattening reduces steric strain in these molecules. Again, these angles are significantly larger for dendrimers with three-fold branches (average values 128–129°) relative to dendrimers with two-fold branches where the average angles range from 115–119°.

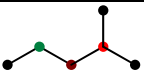
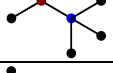
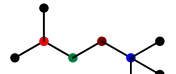
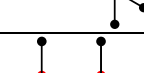
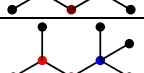
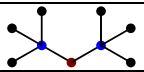
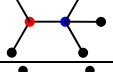
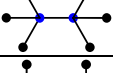
## 5. NMR-Spectroscopy

The structural analysis of polysilane dendrimers in solution by means of  $^1\text{H}$ - and  $^{13}\text{C}$ -NMR spectroscopy is complicated by the extremely narrow chemical shift window in which the hydrogen and carbon nuclei of methylsilyl groups usually appear.  $^{29}\text{Si}$ -NMR, however, is a much more useful spectroscopic tool because of a variety of differently substituted silicon nuclei present in polysilanes dendrimers that can appear at significantly different chemical shifts. For example, there can be four types of silicon nuclei,  $[\text{Si}]$ , in permethylated branched polysilanes that differ in  $\alpha$ -substitution; primary  $[\text{R}_3\text{Si}(\text{Si})]$ , secondary  $[\text{R}_2\text{Si}(\text{Si})_2]$ , tertiary  $[\text{RSi}(\text{Si})_3]$  and quaternary silicon nuclei  $[\text{Si}(\text{Si})_4]$  (R = non-silyl group). Table 2 displays the Si-NMR chemical shifts of secondary ( $\text{S}^\beta$ ), tertiary ( $\text{T}^\beta$ ) and quaternary silicons ( $\text{Q}^\beta$ ) of a series of permethylated linear and branched oligosilanes. The symbols  $\text{S}^\beta$ ,  $\text{T}^\beta$  and  $\text{Q}^\beta$  are used to indicate the number of silicon atoms that are linked to them in  $\alpha$ - and  $\beta$ -position; the symbols S, T and Q for the number of silicons in  $\alpha$ -position and  $\beta$  for the number of silicons in  $\beta$ -position ( $\text{Si-Si}_\alpha\text{-Si}_\beta$ ) [80]. Two opposing chemical shift trends are seen; an up-field shift of the central silicon as the number of  $\alpha$ -silicons increases and a down-field shift as the number of  $\beta$ -silicons increases [81]. The influence of  $\beta$ -silicon on chemical shifts is best seen for secondary silicons (S), which shift from  $-48.6$  ppm for  $\text{S}^0$  to  $-26.0$  ppm for  $\text{S}^6$ . Although not fully consistent, quaternary and tertiary silicons show similar behavior. However, the observation that silicon nuclei in branched and linear polysilanes appear at certain shift windows, ranging from  $-9$  to  $-20$  ppm for primary (P),  $-25$  to  $-50$  ppm for secondary (S),  $-70$  to  $-90$  ppm for tertiary (T) and  $-118$  to  $-136$  ppm for quaternary silicons (Q), allows for the assignment of silicon nuclei just based on their chemical shifts.

**Table 2.**  $^{29}\text{Si}$ -NMR chemical shifts,  $\delta$  [ppm] of selected permethylated branched polysilanes (● = primary silicon; ●/● = secondary silicon; ● = tertiary silicon; ● = quaternary silicon; all methyl groups are omitted for clarity;  $\beta$  refers to the number of silicon nuclei in  $\beta$ -position).

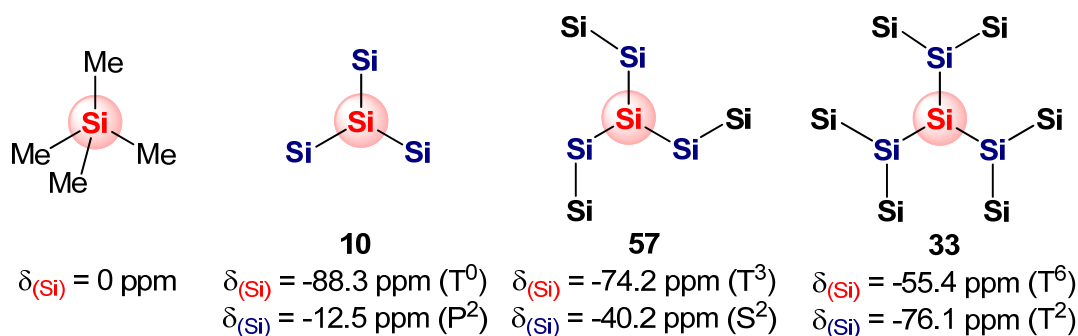
Structure	Solvent	$\delta(\text{Si})$	$\text{T}^\beta$	$\delta(\text{Si})$	$\text{Q}^\beta$	$\delta(\text{Si})$	$\text{S}^\beta$	$\delta(\text{Si})$	$\text{S}^\beta$	Ref.
	$\text{CDCl}_3$	-	-	-	-	-	-	$-48.6$	$\text{S}^0$	[81]
	$\text{CDCl}_3$	-	-	-	-	-	-	$-44.9$	$\text{S}^1$	[81]
	$\text{CDCl}_3$	-	-	-	-	$-43.6$	$\text{S}^1$	$-40.9$	$\text{S}^2$	[81]
	$\text{CDCl}_3$	-	-	-	-	$-43.4$	$\text{S}^1$	$-39.5$	$\text{S}^2$	[81]

Table 2. Cont.

	C <sub>6</sub> D <sub>6</sub>	-88.1	T <sup>0</sup>	-	-	-	-	-	-	[81]
	C <sub>6</sub> D <sub>6</sub>	-	-	-135.5	Q <sup>0</sup>	-	-	-	-	[81]
	C <sub>6</sub> D <sub>6</sub>	-82.8	T <sup>1</sup>	-	-	-42.9	S <sup>1</sup>	-37.4	S <sup>3</sup>	[82]
	CDCl <sub>3</sub>	-	-	-131.9	Q <sup>1</sup>	-	-	-39.8	S <sup>3</sup>	[81]
	THF-D <sub>8</sub>	-82.1	T <sup>1</sup>	-	-	-34.8	S <sup>3</sup>	-	-	[77]
	CDCl <sub>3</sub>	-81.2	T <sup>1</sup>	-128.6	Q <sup>1</sup>	-33.2	S <sup>3</sup>	-31.8	S <sup>4</sup>	[81]
	CDCl <sub>3</sub>	-	-	-126.5	Q <sup>1</sup>	-	-	-29.0	S <sup>4</sup>	[81]
	C <sub>6</sub> D <sub>6</sub>	-81.6	T <sup>1</sup>	-	-	-	-	-33.0	S <sup>4</sup>	[31]
	CDCl <sub>3</sub>	-78.8	T <sup>1</sup>	-126.0	Q <sup>1</sup>	-	-	-29.2	S <sup>5</sup>	[81]
	CDCl <sub>3</sub>	-	-	-118.2	Q <sup>1</sup>	-	-	-26.0	S <sup>6</sup>	[81]
	CDCl <sub>3</sub>	-81.4	T <sup>2</sup>	-	-	-	-	-	-	[81]
	CDCl <sub>3</sub>	-79.8	T <sup>3</sup>	-129.4	Q <sup>2</sup>	-	-	-	-	[81]
	CDCl <sub>3</sub>	-	-	-130.0	Q <sup>3</sup>	-	-	-	-	[81]
	CDCl <sub>3</sub>	-78.7 -71.4	T <sup>2</sup> T <sup>4</sup>	-	-	-	-	-	-	[23]

Similar shifts but at slightly lower field are observed for dendritic polysilanes ranging from  $-9$  ppm to  $-12$  ppm for primary silicon (P),  $-24$  ppm to  $-32$  ppm for secondary silicon (S),  $-35$  ppm to  $-80$  ppm for tertiary silicon (T) and  $-112$  ppm to  $-128$  ppm for quaternary silicon (Q). Again, the broad ranges seem to depend primarily on the number of  $\alpha$ - and  $\beta$ -silicon atoms, causing opposing chemical shift trends. These trends are nicely reflected in a series of branched and dendritic polysilanes shown in Figure 19. Thus, the central tertiary silicon core experiences a strong down-field shift as more silicon atoms are added in  $\beta$ -position from  $-88.3$  ppm for T<sup>0</sup> to  $-55.4$  ppm for T<sup>6</sup>, while the silicon atoms next to it (shown in blue) are shifted up-field as the number of  $\alpha$ -silicon atoms increases from  $-12.5$  ppm for P<sup>2</sup> to  $-76.1$  ppm for T<sup>2</sup>. Table 3 summarizes the chemical shifts of all known permethylated polysilane dendrimers with no spacer between core and branch point along with some selected branched polysilanes for comparison. Again, progressive down-field shifts are observed for the silicon cores, branch points and spacer (between cores!) upon adding silicon atoms in positions  $\beta$  to them.

**Figure 19.** NMR chemical shift trends for selected permethylated branched and dendritic polysilane **33** (red = central silicon, blue =  $\alpha$ -silicon, black =  $\beta$ -silicon, all methyl groups are omitted for clarity).



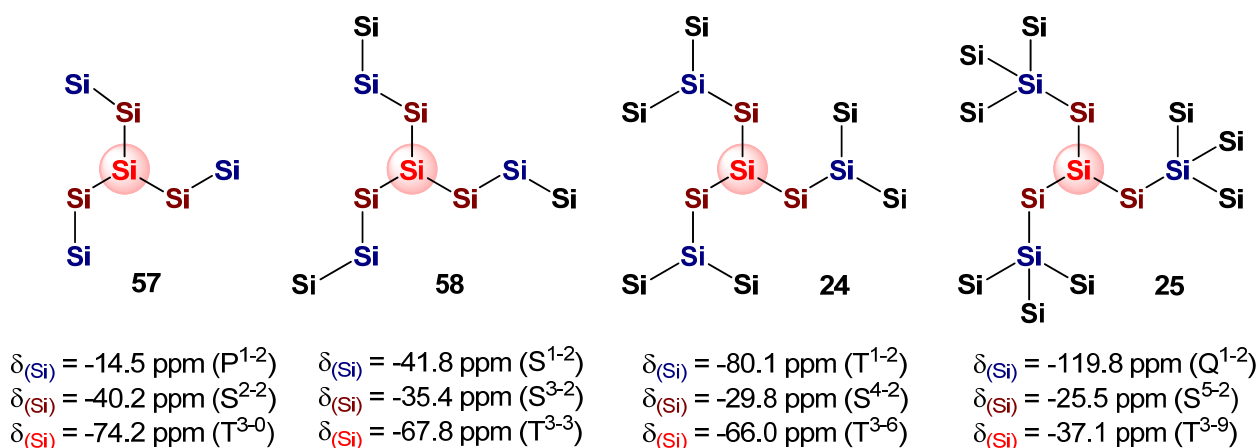
**Table 3.**  $^{29}\text{Si}$ -NMR chemical shifts,  $\delta$  [ppm] of selected permethylated branched and dendritic polysilanes with no spacer between core and branch point (● = core silicon; ● = spacer silicon; ● = branch silicon; ● = primary silicon; all methyl groups are omitted for clarity; the letters  $\beta$  and  $\gamma$  refer to the number of silicon nuclei in  $\beta$ - and  $\gamma$ -positions).

No.	Structure	Solvent	$\delta(\text{Si})$ core	$T^{\beta-\gamma}$	$\delta(\text{Si})$ branch	$T^{\beta-\gamma}$	$\delta(\text{Si})$ spacer	$S^{\beta-\gamma}$	Ref.
10		$\text{CDCl}_3$	-88.3	$T^{0-0}$	-	-	-	-	[81]
		$\text{THF-D}_8$	-82.1	$T^{1-1}$	-	-	-34.8	$S^{3-2}$	[77]
11		$\text{CDCl}_3$	-81.4	$T^{2-0}$	-	-	-	-	[81]
57		$\text{CDCl}_3$	-74.2	$T^{3-0}$	-	-	-40.2	$S^{2-2}$	[33]
52		$\text{C}_6\text{D}_6$	-54.4	$T^{5-1}$	-76.8	$T^{2-3}$	-31.4	$S^{3-6}$	[37]
33		$\text{C}_6\text{D}_6$	-55.4	$T^{6-0}$	-76.1	$T^{2-4}$	-	-	[31]
51		$\text{CDCl}_3$	-43.8	$T^{6-4}$	-74.8	$T^{2-4}$	-	-	[21]

Careful analysis of the  $^{29}\text{Si}$ -NMR data of all known polysilanes dendrimers by Krempner *et al.* revealed that the chemical shifts of the silicon nuclei also depend on the number of silicon atoms in  $\gamma$ -positions in addition to the number of  $\alpha$ - and  $\beta$ -silicons ( $\text{Si-Si}_\alpha\text{-Si}_\beta\text{-Si}_\gamma$ ) [48]. It was also noticed that the number of silicon nuclei in  $\gamma$ -position relative to central tertiary silicon core (T) can have a pronounced effect on its chemical shift and that in all polysilane dendrimers the chemical shifts of the tertiary silicon cores (T), tertiary or quaternary branch points (T, Q) and secondary silicon spacers (S)

are progressively down-field shifted upon increasing the number of silicon nuclei in  $\gamma$ -positions (Figure 20 and Table 4). The impact of all three types of silicons ( $\alpha$ ,  $\beta$ ,  $\gamma$ ) on the chemical shift trends clearly appears for a series of selected branched polysilanes and dendritic polysilanes shown in Figure 20. First, the  $T^{3-\gamma}$  silicons (shown in red) are progressively down-field shifted as the number of  $\gamma$ -silicons increases (from 0 to 9), while the  $S^{\beta-2}$  silicons (shown in brown) are shifted to lower field with increasing number of  $\beta$ -silicons (from 2 to 5). In contrast, the silicon nuclei shown in blue—all have the same number of  $\beta$ - and  $\gamma$ -silicons (1-2)—are tremendously up-field shifted as the number of  $\alpha$ -silicons increases (from P to Q). Table 3 summarizes the chemical shifts of all known permethylated polysilane dendrimers with spacers between core and branch point along with some selected branched polysilanes for comparison. Again, progressive down-field shifts are observed for the silicon cores, branch points and spacer upon adding silicons in  $\beta$ - and  $\gamma$ -positions to them.

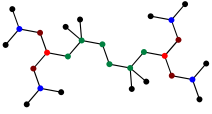
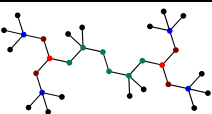
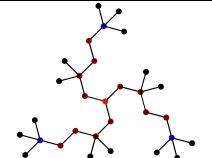
**Figure 20.** NMR chemical shift trends for selected permethylated branched and dendritic polysilanes (red = central silicon, brown =  $\alpha$ -silicon, blue =  $\beta$ -silicon, black =  $\gamma$ -silicon; all methyl groups are omitted for clarity).



**Table 4.**  $^{29}\text{Si}$ -NMR chemical shifts [ppm] of selected branched and dendritic polysilanes [ $\bullet$  = core silicon;  $\bullet/\bullet$  = spacer silicon;  $\bullet$  = branch silicon;  $\bullet$  = primary silicon; the letters  $\beta$  and  $\gamma$  refer to the number of silicon nuclei in  $\beta$ - and  $\gamma$ -position].

No.	Structure	Solvent	$\delta(\text{Si})$	$T^{\beta-\gamma}$	$\delta(\text{Si})$	$Q^{\beta-\gamma}$	$\delta(\text{Si})$	$S^{\beta-\gamma}$	Ref.
57		$\text{CDCl}_3$	-74.2	$T^{3-0}$	-	-	-40.2	$S^{2-2}$	[33]
58		$\text{C}_6\text{D}_6$	-67.8	$T^{3-3}$	-	-	-41.8 -35.4	$S^{1-2}$ $S^{3-2}$	[45]
54		$\text{C}_6\text{D}_6$	-80.0 -64.6	$T^{1-2}$ $T^{3-5}$	-	-	-30.0 -31.7	$S^{4-2}$ $S^{3-4}$	[44]
24		$\text{C}_6\text{D}_6$	-80.1 -66.0	$T^{1-2}$ $T^{3-6}$	-	-	-29.8	$S^{4-2}$	[45]
47		$\text{CDCl}_3$	-80.1 -64.8 -62.3	$T^{1-2}$ $T^{3-6}$ $T^{3-6}$	-	-	-30.0 -26.7	$S^{4-2}$ $S^{4-4}$	[20]

Table 4. Cont.

40		C <sub>6</sub> D <sub>6</sub>	-78.3 -59.9	T <sup>1-2</sup> T <sup>3-7</sup>	-123.0	Q <sup>1-2</sup>	-29.3 -25.1	S <sup>4-2</sup> S <sup>5-2</sup>	[45]
55		C <sub>6</sub> D <sub>6</sub>	-78.2 -55.7	T <sup>1-2</sup> T <sup>3-7</sup>	-109.7	Q <sup>2-3</sup>	-28.7 -26.6 -24.7	S <sup>4-2</sup> ? ?	[47]
41		C <sub>6</sub> D <sub>6</sub>	-79.1 -50.8	T <sup>1-2</sup> T <sup>3-8</sup>	-121.8	Q <sup>1-2</sup>	-29.3 -25.2	S <sup>4-2</sup> S <sup>5-2</sup>	[45]
25		CDCl <sub>3</sub>	-37.1	T <sup>3-9</sup>	-119.8	Q <sup>1-2</sup>	-25.5	S <sup>5-2</sup>	[19]
56		C <sub>6</sub> D <sub>6</sub>	-35.3	T <sup>3-9</sup>	-120.9 -109.7	Q <sup>1-2</sup> Q <sup>2-3</sup>	-26.3 -25.7 -25.6	? ? ?	[47]
26		CDCl <sub>3</sub>	-30.3	T <sup>3-9</sup>	-126.8 -110.0	Q <sup>1-1</sup> Q <sup>2-3</sup>	-28.5 -27.0 -25.0	? ? ?	[84]
53		C <sub>6</sub> D <sub>6</sub>	-77.9 -55.1	T <sup>1-2</sup> T <sup>4-6</sup>	-	-	-28.6	S <sup>4-3</sup>	[44]

Most remarkable, however, are the extreme down-field shifts upon going from T<sup>3-6</sup> and T<sup>3-7</sup> silicon nuclei (-57 ppm to -66 ppm) to T<sup>3-9</sup> silicon nuclei with values ranging from -30 ppm to -37 ppm [83,84]. These drastic changes in chemical shift seem to originate from dramatic changes in critical bond parameters such as Si-Si distances and Si-Si-Si angles around the central core units, which are only observed for polysilane dendrimers with exclusively three-fold branches (core = T<sup>3-9</sup>). As mentioned before, the strain in these molecules is released by an extreme flattening of the Si-Si-Si angles (core-spacer-branch ~130°) emanating from the central T<sup>3-9</sup> core and an elongation of the spacer-branch Si-Si distances (239–240 pm). Therefore, it is reasonable to assume that these drastic chemical shift changes are a result of both electronic (increased number of electropositive silicon nuclei) and steric effects (changes in the overall geometry). Note, however, that the spacer silicon nuclei (S<sup>β-γ</sup>), which are most affected by these changes in geometry are only slightly down-field shifted upon increasing the number of silicon nuclei in β-positions.

To summarize, the empirical <sup>29</sup>Si-NMR chemical shift ranges of branched and linear polysilanes quoted in Table 2 provide a useful basis for the assignment of <sup>29</sup>Si resonances to the various silicons in single-core and double-core dendrimers. Moreover, application of an extended empirical model that considers the impact of silicon nuclei in γ-positions (γ-silicons) on the Si-NMR chemical shift allowed for differentiation between tertiary silicons being the central cores and tertiary silicon being the branch points. The observed ranges for secondary spacer silicons (S<sup>β-γ</sup>), however, are too small to be useful in terms of assigning <sup>29</sup>Si resonances to certain secondary silicons within the large dendritic molecules **55** and **56**. As suggested by Lambert *et al.* [25], an unambiguous assignment to specific silicon nuclei can only be achieved by carrying out <sup>29</sup>Si-<sup>29</sup>Si 2D INADEQUATE-NMR spectroscopy, which provides

proof for sequential connectivities of Si-Si bonds in all structural types of polysilanes, although it is a time-consuming experiment (*ca.* 4 days).

## 6. Electronic Properties

### 6.1. General Remarks

One of the most characteristic features of polysilanes, regardless of whether they are linear, branched, hyperbranched or dendritic in structure, is the extensive delocalization of  $\sigma$ -bonded electrons ( $\sigma$ -conjugation) along silicon chains, resulting in strong electronic absorptions in the near UV due to a  $\sigma$ - $\sigma^*$  transition [1–3]. Both intensity and energy of the absorption are extremely sensitive to the overall conformation and the number of silicon atoms in the longest silicon chain [1–3] as well as the electronic and steric nature of the attached substituents [85–89]. For example, in linear permethylated polysilanes of general formula  $\text{Me}(\text{SiMe}_2)_n\text{Me}$  [90–93] delocalization of  $\sigma$ -electrons along the silicon chain leads to UV absorption that increases in wavelength and intensity as the number of silicon atoms in the polysilane chain increases with a wavelength reaching an asymptotic value of around 293 nm for  $[\text{Me}(\text{SiMe}_2)_{24}\text{Me}]$  (see also Figure 21 (left)).

**Figure 21.** (left) UV absorption maxima  $[\lambda_{\text{max}}]$  as a function of the number of silicon atoms of the silicon chain of linear polysilanes with general formula,  $\text{Me}(\text{SiMe}_2)_n\text{Me}$  (measured at room temperature in solution); (right) UV absorption maxima  $[\lambda_{\text{max}}]$  of the permethylated polysilane dendrimers **24-26**, **41**, **44**, **47** and **51-56** as a function of the number of silicon atoms of the longest silicon chain (measured at room temperature in solution).

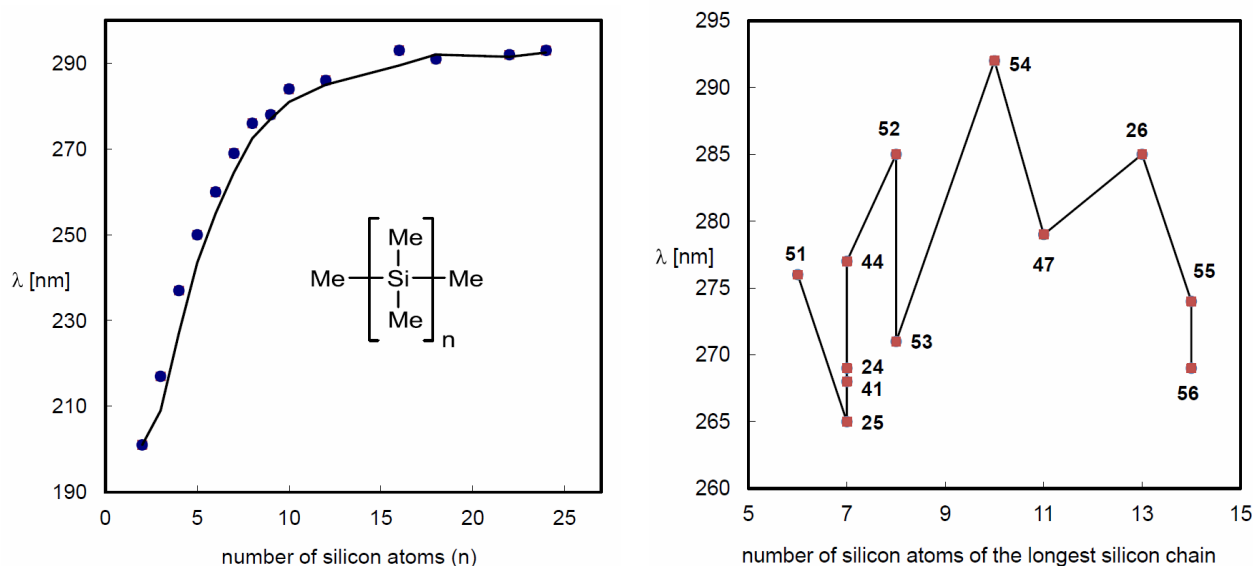


Table 5 and Figure 21 (right) summarize the electronic absorption data for dendritic polysilanes. The data show that only the extinction coefficient for permethylated polysilane dendrimers tends to increase as the total number of silicon atoms and the number of silicon atoms in the longest chain increase from  $3.4 \times 10^4$  to  $13.0 \times 10^4$ . The intensity of the UV absorption maximum is stronger in polysilane dendrimers than in linear polysilanes, primarily because of the higher “concentration” of

silicon chains. Accordingly, the permethylated single-core polysilane dendrimers with longest chains of 7 silicon atoms **24**, **25**, **40** and **41** exhibit similar extinction coefficients and absorption maxima ranging from  $0.5$  to  $0.6 \times 10^5$  and from 265 to 269 nm, respectively. However, unlike in linear polysilanes there is no correlation between the energy of the absorption maximum and the number of silicon atoms in the longest chain for permethylated polysilane dendrimer. For example, comparison of UV data of the single-core dendrimers **44** with **40**, both have a total number of 14 silicon atoms and longest chains of 7 silicon atoms shows that the absorption maximum of **44** is red shifted by *ca.* 8 nm relative to **40**. Furthermore, double-core dendrimer **52** with a longest chain of only 8 silicon atoms displays an absorption maximum at 285 nm, whereas **56** absorbs at only 269 nm even though it is the largest polysilane dendrimer reported to date with longest chains of 14 silicon atoms and a total of 32 silicon atoms per molecule. Clearly, there are other factors such as conformational arrangements, steric and electronic effects that may influence the electronic properties of polysilane dendrimers.

**Table 5.** UV absorption spectra of permethylated single-core and double-core polysilane dendrimers (● = core silicon; ●/● = spacer silicon; ● = branch silicon; ● = primary silicon; all methyl groups are omitted for clarity).

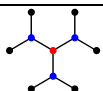
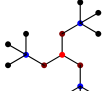
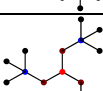
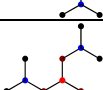
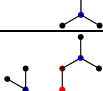
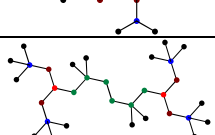
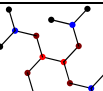
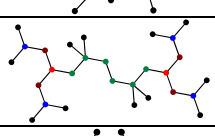
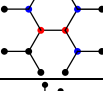
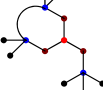
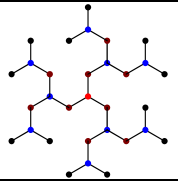
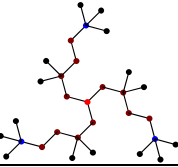
No.	Structure	Dendrimer type	$\lambda_{\max}$ (nm)	$\epsilon$ ( $10^4$ )	No. of Si atoms of the longest Si chain	Total no. of Si atoms	Ref.
33		S-1302	240	3.4	5	10	[31]
25		S-1313	265	5.2	7	16	[47]
41		irregular	268	5.9	7	15	[47]
24		S-1312	269	5.0	7	13	[47]
40		irregular	269	6.0	7	14	[45]
56		D-1213-6	269	13.0	14	32	[47]
53		D-1212-0	271	8.2	8	18	[44]
55		D-1212-6	274	13.0	14	28	[47]
51		D-1202-0	276	2.3	6	14	[21]
44		irregular	277	6.0	7	14	[45]

Table 5. Cont.

47		S-2312	279	9.6	11	31	[20]
52		D-1202-2	285	5.6	8	16	[37]
26		S-1343	285	12.0	13	31	[24]
54		D-1212-2	292	5.5	10	20	[44]

## 6.2. Conformational Effects

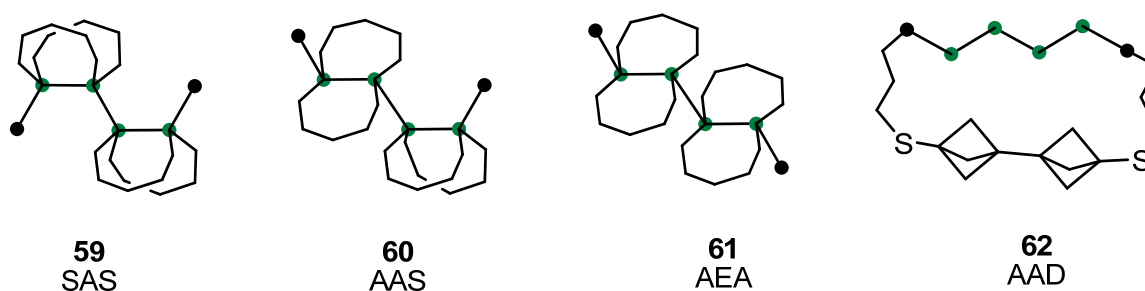
Peralkylated linear polysilanes can adopt various conformational arrangements that deviate from the two preferred *CCCC* dihedral angles  $\omega$  in hydrocarbons,  $180^\circ$  (A, anti) and  $60^\circ$  (gauche, G). Deviations from these angles can reasonably be explained by repulsive interaction between substituents attached to the silicon silicon backbone, which increase as the size of the substituents is increased relative to the Si-Si bond length [94,95]. Steric effects are also responsible for the observation of three conformational families of dihedral angles: *gauche* (G,  $\omega \sim 60^\circ$ ), *ortho* (O,  $\omega \sim 90^\circ$ ) and *anti* (A,  $\omega \sim 180^\circ$ ) dominating in linear polysilanes [96–98]. Even more conformers are possible in branched and dendritic polysilanes due to the redundancy of silicon-silicon chains combined with strongly repulsive interactions between substituents. Possible conformers in polysilane dendrimers can be classified according to their *SiSiSiSi* dihedral angles as syn (S,  $\omega \sim 0^\circ$ ), cis (C,  $\omega \sim 30^\circ$ ), gauche (G,  $\omega \sim 60^\circ$ ), ortho (O,  $\omega \sim 90^\circ$ ), eclipsed (E,  $\omega \sim 120^\circ$ ), deviant (D,  $\omega \sim 150^\circ$ ) and anti (A,  $\omega \sim 180^\circ$ ).

Recent studies on permethylated linear polysilanes with discrete conformations have revealed the great impact of the overall silicon chain conformation on the degree of  $\sigma$ -conjugation and the UV spectroscopic properties. It was shown theoretically and experimentally that the  $\sigma$ - $\sigma^*$  absorption peak shifts dramatically to the red as the *SiSiSiSi* dihedral angle,  $\omega$ , is increased from  $0^\circ$  to  $180^\circ$  [99–104]. This effect was explained by 1,4-orbital interactions ( $\beta_{vic}$ ), being most effective (maximum orbital overlap) in the HOMO ( $\sigma$ -type orbital) of a syn-conformer, while not present in an anti-conformer. In fact, the 1,4-orbital interaction in syn-conformers lowers the energy of the HOMO ( $\sigma$ -orbital) and consequently increases the energy of the  $\sigma$ - $\sigma^*$  transition relative to that of the anti-conformer ([99] and references cited therein).

Perhaps, the most striking example provides a series of conformationally constrained hexasilanes **59–62** (composed of three dihedral angles) that have been structurally characterized by X-ray studies [100,101] (Figure 22). Within this series of hexasilanes both absorption maximum and extinction coefficient monotonically increase as the *SiSiSiSi* dihedral angles become larger from SAS ( $\lambda = 239$  nm,

$\varepsilon = 1.9 \times 10^4$ ), AAS ( $\lambda = 255$  nm,  $\varepsilon = 3.1 \times 10^4$ ), AEA ( $\lambda = 259$  nm,  $\varepsilon = 5.4 \times 10^4$ ) to AAD ( $\lambda = 267$  nm,  $\varepsilon = 6.7 \times 10^4$ ) (Figure 22). These findings clearly revealed that  $\sigma$ -conjugation in polysilanes is effectively extended by *anti* or *deviant* conformations, while conformations with small dihedral angles such as *syn*, *cis* or *gauche* do not contribute to the extent of  $\sigma$ -conjugation [102].

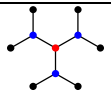
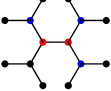
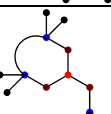
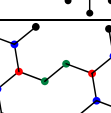
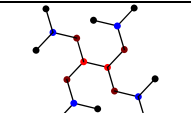
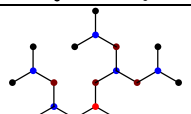
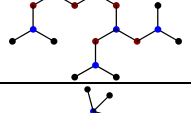
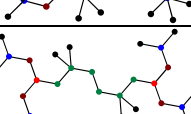
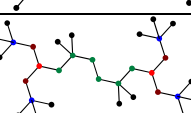
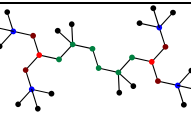
**Figure 22.** Structure and conformation of selected hexasilanes with rigid silicon chains (● = secondary silicon; ● = primary silicon; all methyl groups are omitted for clarity).



Similar conclusions can be drawn for polysilane dendrimer, even though the redundancy of silicon chains and the steric strain causes a variety of more or less flexible conformers to be formed, each contributing differently to the extent of  $\sigma$ -conjugation along the silicon backbone. The presence of these different conformers complicates analysis and assignment of the often broad and intense UV absorption bands and hampers deducing the relationship between conformation and photophysical properties. Moreover, dihedral angles such as *ortho* are common in dendritic structures and it is not clear yet to what extent *ortho* conformers would contribute to the degree of  $\sigma$ -conjugation along silicon chains. Table 6 summarizes the overall conformation and average silicon-silicon distances of the longest silicon chains in selected polysilane dendrimers obtained from the X-ray data along with the measured UV absorption maxima. Note, that the average silicon-silicon distances of the longest silicon chains of all structurally characterized polysilane dendrimers (except for **51**) lie within the relatively narrow range of 236–238 pm, suggesting only minimal influence of silicon-silicon bond stretching on the energy of the  $\sigma$ - $\sigma^*$  transition [105] and allowing for comparison of both conformational arrangements and UV absorption characteristics of individual dendrimers with each other.

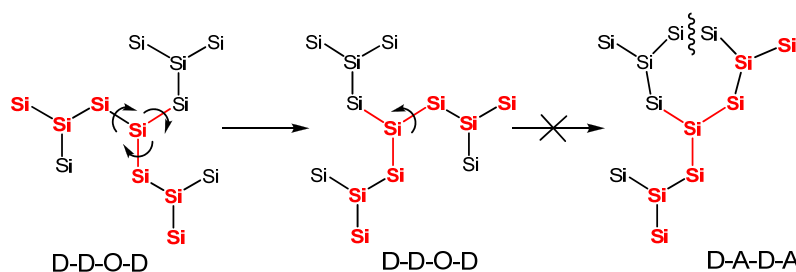
The longest silicon chains in the single-core dendrimers **24**, **40** and **25** contain seven silicon atoms (heptasilane chain) and are defined by four tetrasilane dihedral angles. The conformational analysis revealed that conformers with exclusively large dihedral angles such as all-*anti* (*A-A*) or all *deviant* (*D-D*) or mixed *A-D* segments exist only in several pentasilane subunits and that in most of the heptasilane chains *anti* (*A*) or *deviant* (*D*) segments are interrupted by additional *ortho* (*O*) or *gauche* (*G*) conformers, which are predicted to interrupt  $\sigma$ -conjugation along the chain. The observed conformational arrangements (DDOD, ADOD etc.) can be explained in terms of the bulkiness of the dendrimer wings. They are oriented in the same direction (clockwise or anti-clockwise), which reduces their repulsive interactions (see also Figure 18). In all three dendrimers, however, the heptasilane chains with largest dihedral angles are fairly similar to each other, which correlate with the similar UV spectroscopic data of **24**, **40** and **25**.

**Table 6.** UV absorption maxima of polysilane dendrimers and conformations of silicon chains with largest *Si-Si-Si-Si* dihedral angles (*A*,  $\omega \sim 180^\circ$ ; *D*,  $\omega \sim 150^\circ$ ; *E*,  $\omega \sim 120^\circ$ ; *O*,  $\omega \sim 90^\circ$ ; *G*,  $\omega \sim 60^\circ$ ; *C*,  $\omega \sim 30^\circ$ ) and average Si-Si distances [pm] thereof (● = core silicon; ●/● = spacer silicon; ● = branch silicon; ● = primary silicon).

No.	Structure	$\lambda_{\max}$ [nm]	No. of chain Si	Conformation (X-ray)	Av. Si-Si distance	Ref.
33		240	5	OA	236.0	[31]
51		276	6	EAE	238.6	[21]
25		265	7	DAGD	235.7	[47]
24		269	7	DDOD	235.8	[47]
40		269	7	ADOD	237.4	[45]
			7	DDOD	236.9	
44		277	7	ADAD	237.0	[45]
52		285	8	DEDED	237.2	[37]
53		271	8	DDCDD	237.3	[44]
			7	DDOD	237.2	
47		279	11	DDODODOD	237.6	[20]
			7	DDOD	236.7	
26		285	13	ADGCAGGGDA	237.1	[24]
55		274	14	DDOAGDGAODD	237.7	[47]
			7	DDOD	236.1	
56		269	14	DAGOGDGOGAD	238.2	[47]
			7	DAGD	237.7	

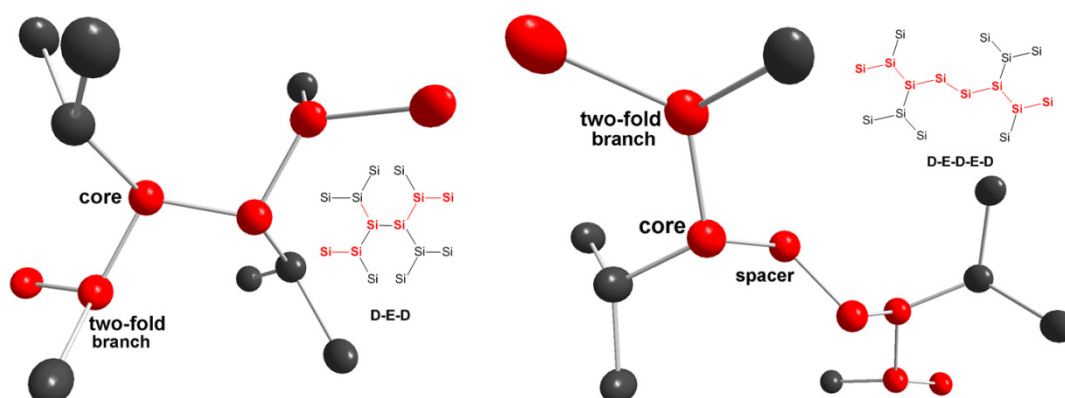
The strong impact of the silicon chain conformation on the energy of the UV absorption maxima of this class of single-core dendrimers is best demonstrated by comparing dendrimer **40** with conformationally constrained dendrimer **44**; both have longest heptasilane chains and the same total number of silicon atoms in the molecule [45]. Assuming that the absorption maximum originates from silicon chains with largest dihedral angles, **44** is red-shifted by 8 nm as a result of a conformational change from a ADOD conformer in **40** to a ADAD conformer in **44**. Clearly this conformational arrangement can only be enforced by connecting two of the three dendrimer wings with an alkylene linker as is the case for **44**. The formation of all-anti or all-deviant conformers in unconstrained single-core dendrimers is not preferred, since this would lead to considerable repulsions of the bulky wings as shown in Figure 23.

**Figure 23.** Conformations of heptasilane chains in **24** (shown in red) [all methyl groups are omitted for clarity].



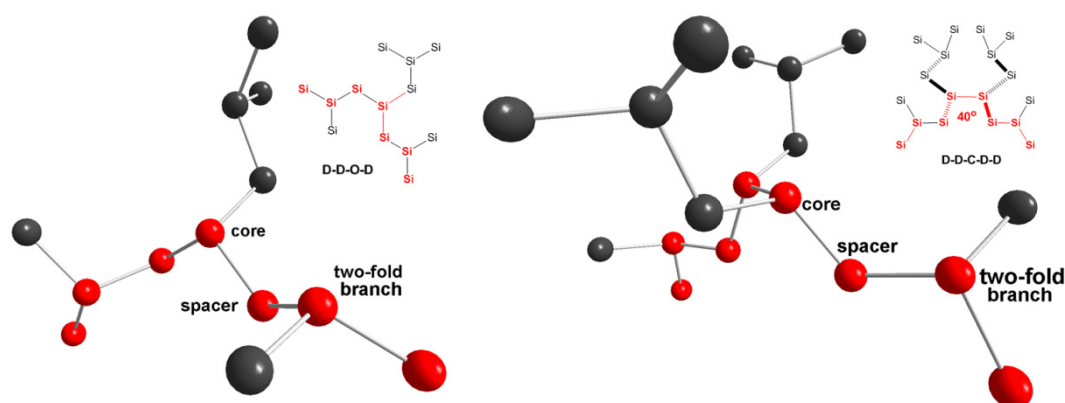
Notably, the broad and intense absorption maxima of the majority of double-core polysilane dendrimers are at lower energy than to those of single-core dendrimers with comparable silicon chain length. Most remarkable in this respect are the double-core dendrimers **51** (longest hexasilane chain;  $\lambda_{\max} = 276$  nm), **52** (longest octasilane chain;  $\lambda_{\max} = 285$  nm) both being characterized by X-ray crystallography and **54** (longest decasilane chain;  $\lambda_{\max} = 292$  nm); the latter with the longest wavelength of all known permethylated polysilane dendrimers. The conformational analysis (from the X-ray data) reveals that the *SiSiSiSi* dihedral angles in at least one of the longest hexasilane and octasilane chains of the double-core species **51** (EAE) and **52** (DEDED) (Figure 24), respectively, are larger than any of the longest heptasilane and undecasilane chains of the single-core species **24** (DDOD) (Figure 24) and **47** (DDODODOD), respectively.

**Figure 24.** Solid-state structures of the double-core dendrimers **51** (left) and **52** (right) (all H and C atoms omitted for clarity; longest silicon chains with largest dihedral angles are shown in red).



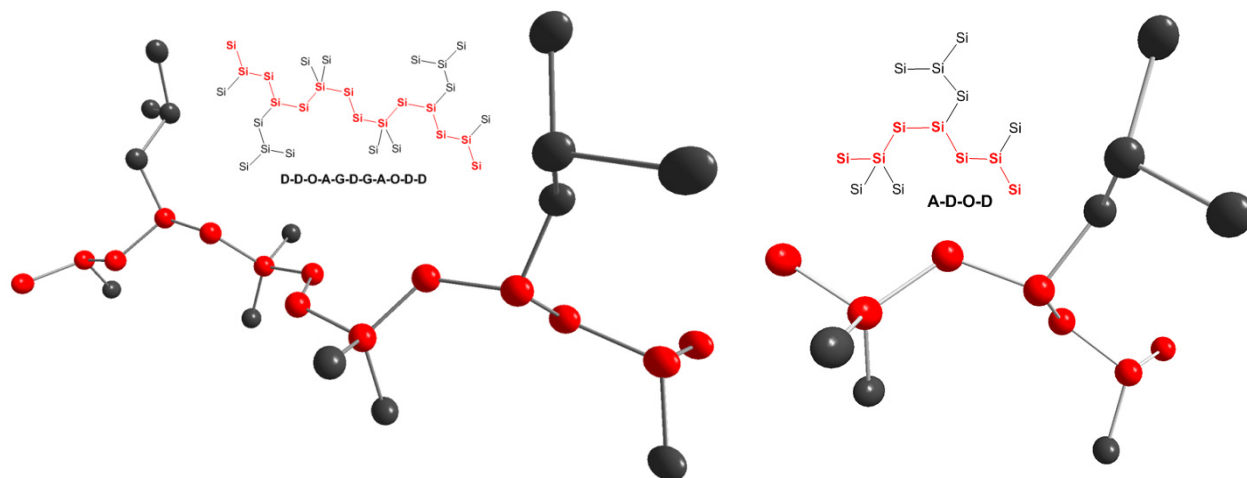
On the other hand, the absorption maximum of double-core dendrimer **53** ( $\lambda_{\max} = 271$  nm) is only slightly shifted to the red relative to single-core dendrimer **24** ( $\lambda_{\max} = 269$  nm). Again, the X-ray data of **53** revealed that conformers with all-deviant segments exist only in several pentasilane subunits and that in the octasilane chains deviant (*D*) segments are interrupted by additional ortho (*O*) or even cis (*C*) conformers. Thus, it seems that in this type of dendrimer the  $\sigma$ -electrons are fully delocalized along the dendrimer wings (dendrons), which, similar to **24**, have longest chains of 7 silicon atoms and DDOD conformations (Figure 25). The observation that the double-core dendrimers **52** and **54** (no X-ray data) absorb at significantly longer wavelengths than **53** implies that the incorporation of silicon spacer groups between the two cores as in **52** and **54** reduces steric repulsion between the dendrimer wings and, consequently, allows for conformations being optimal for the delocalization of  $\sigma$ -electrons along the silicon main chains.

**Figure 25.** Solid-state structures of single-core dendrimer **24** (left) and double-core dendrimer **53** (right) [all H and C atoms are omitted for clarity; longest silicon chains with largest dihedral angles are shown in red].



Another striking example, which emphasizes the importance of conformational effects with regard to the degree of  $\sigma$ -conjugation, is provided by the double-core dendrimers **55** and **56** (Figure 26). According to the X-ray data, **55** has longest chains of 14 silicon atoms but conformers with exclusively large dihedral angles such as all-anti or all-deviant segments exist only in several hexa- and pentasilane subunits, which are interrupted by additional ortho (*O*) or gauche (*G*) units. Note, however, that the heptasilane subunits of the dendrimer wings of **55** (DDOD) have dihedral angles fairly similar to those of the irregular single-core dendrimer **40** (DAGD and DDOD). In fact, **55** may be described as a dimer of **40**: dendrimer **55** has a total of 28 silicon atoms, whereas **40** is composed of 14 silicon atoms. Accordingly, the wavelengths of UV absorption maxima **55** ( $\lambda = 274$  nm) and **40** ( $\lambda = 269$  nm) are similar to each other, but the extinction coefficients differ by a factor of two (**40**,  $\epsilon = 0.6 \times 10^5$ ; **55**,  $\epsilon = 0.6 \times 10^5$ ). Clearly, these examples show that it is primarily the conformation of the silicon chain that determines the optical properties of polysilane dendrimers.

**Figure 26.** Solid-state structures of double-core dendrimer **55** (left) and irregular single-core dendrimer **40** (right) (all H and C atoms omitted for clarity; longest silicon chains with largest dihedral angles are shown in red).



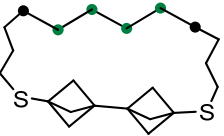
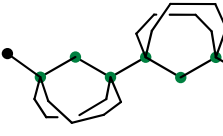
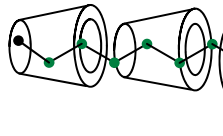
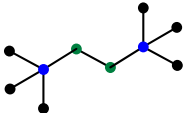
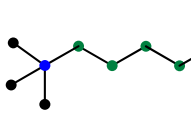
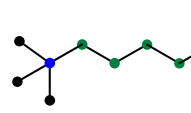
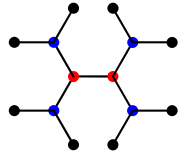
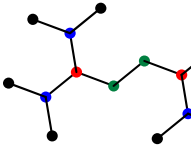
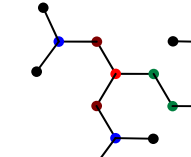
### 6.3. Conformation and $\sigma$ -conjugation in Dendritic, Branched and Linear Structures

From the discussion above it seems to be clear that the silicon backbone conformation is one of the major factors in determining the degree of  $\sigma$ -conjugation not only in linear polysilanes but also in branched and dendritic structures. For comparison, the silicon backbone conformations and average silicon-silicon distances, derived from X-ray diffraction data and the UV absorption data of linear, branched and dendritic polysilanes of chain lengths 6, 8 and 10 are summarized in Table 7.

Linear permethylated polysilanes can adopt various silicon chain conformations in solution primarily due to the low rotational barriers of the silicon-silicon bonds. As a result, mixtures of twisted conformers are observed in solution causing relatively broad UV absorption bands at room temperature. Upon cooling to 77 K, however, the absorption maxima of these linear oligosilanes are significantly red-shifted and the absorption bands become sharper due to a conformational transition from twisted to predominantly helical all-anti conformers, meant to be optimal for  $\sigma$ -conjugation.

Evidence that a transition from twisted to all-trans conformers is responsible for the observed red-shift of the absorption maxima upon cooling to 77 K was provided by the synthesis and UV spectroscopic measurements of conformationally rigid linear oligosilanes with exclusively large dihedral angles (ideally all-anti). In fact, hexasilane **62** and all-anti octasilane **63**, reported by Michl [100] and Tamao [103] *et al.*, respectively, and decasilane/cyclodextrin inclusion complex **64**, reported by Kira's group [106], display absorption maxima at room temperature that have the longest wavelengths and the highest extinction coefficients within the series of linear hexa- octa- and decasilanes.

**Table 7.** UV absorption data (in solution) and critical structural parameters of the longest silicon chains of selected permethylated linear, branched and dendritic polysilanes (*A*,  $\omega \sim 180^\circ$ ; *D*,  $\omega \sim 150^\circ$ ; *E*,  $\omega \sim 120^\circ$ ; ● = core silicon; ●/● = spacer silicon; ● = branch silicon; ● = primary silicon; all methyl groups are omitted for clarity).

Types of polysilanes	no. of chain Si 6	no. of chain Si 8	no. of chain Si 10
<b>linear</b>			
$\lambda_{\max}/\text{nm}$ (293 K)	260	276	284
$\varepsilon/10^4$	2.3	3.0	4.6
$\lambda_{\max}/\text{nm}$ (77 K)	265	282	294
$\varepsilon/10^4$	6.8	13.4	16.0/12.5
Ref.	[90]	[90]	[90,106]
<b>linear with rigid conformation</b>			
	<b>62</b>	<b>63</b>	<b>64</b>
conformation	DAA	AAAAA	-
av. Si-Si distance [pm]	235.0	234.9	-
$\lambda_{\max}/\text{nm}$	267	288	299
$\varepsilon/10^4$	6.7	10.0	15.0
Ref.	[100]	[103]	[106]
<b>branched</b>			
	<b>21</b>	<b>65</b>	<b>66</b>
conformation	DAD	DDADD	DADDADD
av. Si-Si distance [pm]	236.8	236.7	236.1
$\lambda_{\max}/\text{nm}$	257	280	294
$\varepsilon/10^4$	6.6	12.0	6.9
Ref.	[107,108]	[108,109]	[108]
<b>dendritic</b>			
	<b>51</b>	<b>52</b>	<b>54</b>
conformation	EAE	DEDED	-
av. Si-Si distance [pm]	238.6	237.2	-
$\lambda_{\max}/\text{nm}$	276	285	292
$\varepsilon/10^4$	2.3	5.6	5.5
Ref.	[21]	[37]	[44]

Comparing the structural and electronic properties of these linear polysilanes with their branched and dendritic counterparts appears to be difficult as significant steric strain is introduced upon adding silyl groups to the inner silicons of the silicon main chain as is the case in branched and dendritic

polysilanes. In fact, the introduction of further branch points leads to significant deviations of the Si-Si-Si angles from the ideal tetrahedral angles (see also discussion in section 4) and an increase of the average silicon-silicon distances of the longest silicon chains from *ca.* 235 pm for linear polysilanes to *ca.* 239 pm for some of the dendritic polysilanes. As demonstrated for various substituted disilanes by Michl *et al.*, changes of the silicon-silicon distances may affect the energy of the  $\sigma$ - $\sigma^*$  transition and consequently the electronic properties of the bulk material quite dramatically [105]. Note, for example, that sterically crowded hexasilane dendrimer **51** (conformation EDE) clearly outperforms the conformationally rigid carbocyclic hexasilane **62** (conformation AAD) by 10 nm with respect to the wavelength of the absorption maximum (see Table 7). On the other hand, the absorption maximum of sterically less crowded octasilane dendrimer **52** (conformation DEDED) is slightly blue-shifted relative to that of all-anti octasilane **63**, but red-shifted relative to that of its branched counterpart **65**. It is also not clear to what extent the conformations of the longest silicon chains found in the solid-state (X-ray diffraction) for branched and dendritic polysilanes will retain in solution. However, according to the UV absorption characteristics of the branched silanes **65** and **66**, there seem to be some control over the conformation in solution as the absorption maxima of both compounds are significantly red-shifted relative to that of the linear silanes Me(SiMe<sub>2</sub>)<sub>8</sub>Me and Me(SiMe<sub>2</sub>)<sub>10</sub>Me at room temperature. Obviously, similar conclusions can be drawn for polysilane dendrimers as steric strain appears to be the dominating factor in terms of controlling certain silicon main-chain conformations of these well-defined molecules in solution.

#### 6.4. Electronic Effects

Recently, the groups of Stueger and Krempner independently investigated the molecular structures and electronic properties of oxo-functionalized cyclohexasilanes and branched heptasilanes [110–115], respectively. Strong electronic coupling of oxygen-containing donor groups such as OR, OH and OSiR<sub>3</sub> with the silicon-silicon backbone ( $\sigma$ -n mixing) was noticed, resulting in a substantial decrease of the optical band gaps of these compounds. The results of DFT calculations revealed that the energy of the HOMO (primarily  $\sigma$ -orbital of silicon backbone) in these compounds is almost unaffected by the introduction of one or even more of oxo group. In the LUMO, however, strong  $\sigma$ -n mixing of the oxygen lone pairs with the  $\sigma$ -orbitals of the silicon-silicon backbone occurs, which significantly lowers the energy of the LUMO relative to that of permethylated cyclohexasilane and branched heptasilane. Thus, the rather unusual electronic spectra of these oxo-functionalized polysilanes can be explained by a symmetry forbidden HOMO-LUMO transition, which causes the red-shifted UV absorption maxima to be reduced in intensity [116,117].

Table 8 summarizes the absorption data for various functionalized and non-functionalized single-core polysilane dendrimers of first generation along with the conformational data. All these dendrimers have the same numbers of silicon atoms in the longest chains, same total numbers of silicon atoms per molecule and fairly similar conformational arrangements. Note, however, that the UV absorption characteristics of **29** and **30** are strikingly different from that of the hydrido-functionalized analogue **27** and permethylated **24**. In fact, replacing the hydride group attached to the central silicon core with either a chlorine atom or an OH group tremendously shifts the absorption maximum to the red by 23 nm for **29** and 41 nm for **30**, coupled with some reduction in intensity. Again, these findings can be

understood as an optical band gap reduction resulting from effective interactions between chlorine or oxygen lone pair ( $n$ ) and the  $\sigma$ -orbitals of the silicon main chains, resulting in HOMO-LUMO transitions that are symmetry forbidden.

**Table 8.** Electronic absorption spectra of selected single-core polysilane dendrimers of first generation (● = core silicon; ● = spacer silicon; ● = branch silicon; ● = primary silicon; all methyl groups are omitted for clarity).

Compound	$\lambda_{\max}$ (nm)	$\epsilon$ ( $10^4$ )	Conformation (X-ray)	Ref.
27 (X = H)	259	6.9	ADOA	[21]
24 (X = Me)	269	5.0	DDOD	[47]
29 (X = Cl)	282	2.7	-	[43]
30 (X = OH)	300	2.0	-	[50]
<i>l,l</i> -32	280 <sup>a</sup>	2.2	DDOD	[42]
<i>l,u</i> -32	282	3.7	DDED	[42]

<sup>a</sup> measured at 70 °C.

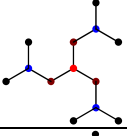
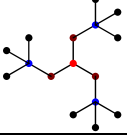
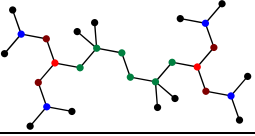
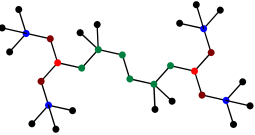
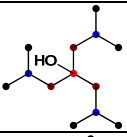
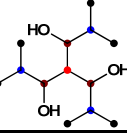
Notably, the absorption maxima of the OH functionalized dendrimers *l,l*-32 and *l,u*-32, each of which has a total number of three OH groups and two OH groups per heptasilane chain, are blue-shifted by *ca.* 20 nm relative to 30, which contains only one OH group attached to the central core silicon. This suggests that the position of the silicon at which the OH group is attached within the silicon chain is more influential in determining the optical band-gaps of these compounds than the absolute number of OH groups attached to the silicon main chain. It seems that strongest electronic coupling of the OH group with the silicon backbone ( $\sigma$ - $n$  mixing) is seen when the OH group is attached to a tertiary silicon atom, whereas secondary and primary Si-OH groups show weaker coupling in the LUMO. This observation is consistent with previous results on the absorption spectra of alkoxy substituted polysilanes of general formula Me-(SiMeOR)<sub>n</sub>-Me and -[Si(OR)<sub>2</sub>]<sub>n</sub>-, in which the OR groups are primarily attached to secondary silicon atoms [87,88]. It is, perhaps, the greater inductive effect associated with the central tertiary silicon compared to secondary or primary silicon atoms, that will more effectively equalize the energies of the oxygen p orbital and silicon main chain  $\sigma$  levels. This would lead to a greater overlap of the involved orbitals resulting in a substantial decrease of the optical band gap [117].

### 6.5. Emissive Properties

The emission properties of linear polysilanes are characterized by sharp emissions in the UV region with a relatively small Stokes shift. Branched polysilanes show a dual emission, one sharp emission at around 360 nm that is assignable to the linear silicon chain and a very broad one in the visible region at around 450 nm, which is related to a branching point (tertiary silicon atom).

Sekiguchi and coworker studied the emissive properties of the first and second generation polysilane dendrimers **24** (S-1312) and **47** (S-2312) at 77 K, and also found for each dendrimer two bands in time-resolved emission spectra [33,36]. From the observed small Stokes shift of the sharp emissions, they concluded that the excitons are fully delocalized over the silicon chains. The broad emission, on the other hand, was thought to be due to excitons that are localized at branching points [Si(Si)<sub>2</sub>]. It was shown that the broad emission arises from an intramolecular energy transfer from the excited state in the silicon chains to that in the branching points. Similar observations were made by Krempner *et al.*, who studied the emissive properties of the permethylated dendrimers **24**, **25**, **40**, **55** and **56** at room temperature, which all showed similarly weak dual emissions (Table 9). Sharp emissions appeared in the UV region at *ca.* 330 nm and broad emissions in the visible region at around 450–460 nm. In the OH-containing dendrimers **30** and *l,l*-**32** the broad emissions at 480 nm (**30**) and 465 nm (*l,l*-**32**) predominated. The most striking feature of **30** and *l,l*-**32**, however, was a marked enhancement of the signal intensity by about a factor of 100 relative to the permethylated counterpart **24**. Interestingly, this behavior closely resembles that of the strongly photoluminescent 2D-siloxene, [Si(OH)<sub>3</sub>H<sub>3</sub>]<sub>n</sub> and its counterpart the 2D-polysilane, [Si<sub>6</sub>H<sub>6</sub>]<sub>n</sub>, which showed a rather weak emission [116,118].

**Table 9.** Emission data of selected polysilane dendrimers (● = core silicon; ●/● = spacer silicon; ● = branch silicon; ● = primary silicon; all methyl groups are omitted for clarity).

No.	Structure	Dendrimer type	$\lambda_{em1}$ (nm)	$\lambda_{em2}$ (nm)	$\lambda_{ex}$ (nm)	c (M)	T (K)	Ref.
24		S-1312	~330	455	283	$5 \times 10^{-5}$	298	[50]
25		S-1313	~330	450–460	275	$10^{-5}$	298	[47]
40		irregular	~330	450–460	275	$10^{-5}$	298	[47]
55		D-1212-6	~330	450–460	275	$10^{-5}$	298	[47]
56		D-1213-6	~330	450–460	275	$10^{-5}$	298	[47]
30		S-1312	-	480	310	$5 \times 10^{-5}$	298	[50]
<i>l,l</i> -32		S-1312	-	465	300	$5 \times 10^{-5}$	298	[50]

## 7. Conclusions

The chemistry and properties of single-core and double-core polysilane dendrimers constitute a new class of highly-branched and silicon-rich architectures, which might have the potential to be useful as opto-electronic materials, has been reviewed. These well-defined molecular compounds are thermally robust and soluble in a variety of solvents and display opto-electronic properties that largely depend on the electronic nature of the substituents and the individual conformational arrangements of the various silicon chains realized in these molecules. Notably, in most double-core polysilane dendrimers the degree of delocalization of the  $\sigma$ -bonded electrons ( $\sigma$ -conjugation) is larger than in single-core dendrimers of comparable chain length as reflected in the different UV spectra. Conformations with large  $SiSiSiSi$  dihedral angles optimal for  $\sigma$ -conjugation along silicon chains are only possible in double-core systems, whereas symmetry and steric requirements render those conformational arrangements in single-core dendrimers impossible. The introduction of oxygen-containing functional groups into dendritic polysilanes, regardless of whether they are single- or double core structures, opens new ways of further tuning the opto-electronic properties of these molecules for materials applications. However, efficient synthetic methods to functionalized polysilane dendrimers of higher generation in high yields still need to be developed.

## Acknowledgments

The support of this work by Texas Tech University is greatly acknowledged.

## References

1. Miller, A.D.; Michl, J. Polysilane high polymers. *Chem. Rev.* **1989**, *89*, 1359–1410.
2. West, R. Polysilanes. In *The Chemistry of Organic Silicon Compounds*; Patai, S., Rappoport, Z., Eds.; Wiley: Chichester, UK, 1989; pp. 1207–1240.
3. Koe, J.R. Organopolysilanes. In *Comprehensive Organometallic Chemistry III*; Crabtree, R.H., Mingos, D.M.P., Eds.; Elsevier Science Ltd.: Oxford, UK, 2006; Volume 3, pp. 549–650.
4. Wilson, W.L.; Weidman, T.W. Excited-state dynamics of one- and two-dimensional  $\sigma$ -conjugated silicon frame polymers: Dramatic effects of branching in a series of hexylsilylene-branched poly(hexylmethylsilylene) copolymers. *J. Phys. Chem.* **1991**, *95*, 4568–4572.
5. Watanabe, A.; Miike, H.; Tsutsumi, Y.; Matsuda, M. Photochemical properties of network and branched polysilanes. *Macromolecules* **1993**, *26*, 2111–2116.
6. Maxka, J.; Chrusciel, J.; Sasaki, M.; Matyaszewski, K. Polysilanes with various architectures. *Macromol. Symp.* **1994**, *77*, 79–92.
7. Richter, R.; Roewer, G.; Böhme, U.; Busch, K.; Babonneau, F.; Martin, H.P.; Müller, E. Organosilicon polymers-synthesis, architecture, reactivity and applications. *Appl. Organomet. Chem.* **1997**, *11*, 71–106.
8. Bianconi, P.A.; Weidman, T.W. Poly(n-hexylsilylene): Synthesis and properties of the first alkyl silicon  $[RSi]_n$  network polymer. *J. Am. Chem. Soc.* **1988**, *10*, 2342–2344.
9. Bianconi, P.A.; Schilling, F.C.; Weidman, T.W. Ultrasound-mediated reductive condensation synthesis of silicon-silicon-bonded network polymers. *Macromolecules* **1989**, *22*, 1697–1704.

10. Furukawa, K.; Fujino, M.; Matsumoto, N. Optical properties of silicon network polymers. *Macromolecules* **1990**, *23*, 3423–2426.
11. Watanabe, A.; Matsuda, M. Electrical and optical properties of heat-treated silicon network polymers. *Chem. Lett.* **1991**, 1101–1104.
12. Watanabe, A.; Matsuda, M.; Yoshida, Y.; Tagawa, S. Radical ions of polysilynes, In *Polymeric Materials for Microelectronic Applications*, ACS Symposium Series 1994, Volume 579, 408–424.
13. Watanabe, A.; Ito, O.; Matsuda, M.; Suezawa, M.; Sumino, K. Photodegradation of polysilanes studied by far-infrared spectroscopy. *Jpn. J. Appl. Phys.* **1994**, *33*, 4133–4134.
14. Matsumoto, H.; Miyamoto, H.; Kojima, N.; Nagai, Y. The first bicyclo[2.2.0]hexasilane system: Synthesis of decaisopropylhexasilabicyclo[2.2.0]hexane. *J. Chem. Soc. Chem. Commun.* **1987**, 1316–1317.
15. Watanabe, A.; Fujitsuka, M.; Ito, O.; Miwa, T. Soluble three-dimensional polysilane with organosilicon nanocluster structure. *Jpn. J. Appl. Phys.* **1997**, *36*, L1265–L1267.
16. Watanabe, A.; Fujitsuka, M.; Ito, O.; Miwa, T. Control of silicon dimensionality of polysilanes and their optical properties. *Mol. Cryst. Liq. Cryst.* **1998**, *316*, 363–366.
17. Watanabe, A.; Fujitsuka, M.; Ito, O. Micropatterning of SiO<sub>2</sub> film using organosilicon nanocluster as a precursor. *Thin Solid Film* **1999**, *354*, 13–18.
18. Lambert, J.B.; Pflug, J.L.; Stern, C.L. Synthesis and structure of a dendritic polysilane. *Angew. Chem. (Int. Ed. Engl.)* **1995**, *34*, 98–99.
19. Suzuki, H.; Kimata, Y.; Satoh, S.; Kuriyama, A. Polysilane dendrimer. Synthesis and characterization of [2,2-(Me<sub>3</sub>Si)<sub>2</sub>Si<sub>3</sub>Me<sub>5</sub>]<sub>3</sub>SiMe. *Chem. Lett.* **1995**, 293–294.
20. Sekiguchi, A.; Nanjo, M.; Kabuto, C.; Sakurai, H. polysilane dendrimers. *J. Am. Chem. Soc.* **1995**, *117*, 4195–4196.
21. Lambert, J.B.; Pflug, J.L.; Denari, J.M. First-generation dendritic polysilanes. *Organometallics* **1996**, *15*, 615–625.
22. Suzuki, H.; Kuriyama, A. Branched polysilanes and production thereof. *Jpn. Kokai Tokkyo Koho* **1996**, JP 8073472 A.
23. Herzog, U.; Notheis, C.; Brendler, E.; Roewer, G.; Thomas, B. <sup>29</sup>Si NMR investigations on oligosilane dendrimers. *Fresenius. J. Anal. Chem.* **1997**, *357*, 503–504.
24. Lambert, J.B.; Wu, H. Synthesis and crystal structure of a nanometer-scale dendritic polysilane. *Organometallics* **1998**, *17*, 4904–4909.
25. Lambert, J.B.; Basso, E.; Qing, N.; Lim, S.H.; Pflug, J.L. Two-dimensional silicon-29 inadequate as a structural tool for branched and dendritic polysilanes, *J. Organomet. Chem.* **1998**, *554*, 113–116.
26. Marschner, C.; Hengge, E. Stepwise synthesis of functional polysilane dendrimers. In *Organosilicon Chemistry III: From Molecules to Materials*, 3rd ed.; Auner, N., Weis, J., Eds.; Wiley-VCH Verlag GmbH: Weinheim, Germany, 1998; pp. 333–336.
27. Lambert, J.B.; Liu, X.; Wu, H.; Pflug, J.L. Anionic vs. radical intermediates in the fragmentation reactions of dendritic polysilanes. *J. Chem. Soc. Perkin Trans. 2* **1999**, 2747–2749.

28. Nanjo, M.; Sunaga, T.; Sekiguchi, A.; Horn, E. Crystal structures of the first generation of phenyl-substituted and permethyl-substituted dendritic polysilanes. *Inorg. Chem. Comm.* **1999**, *2*, 203–206.
29. Lambert, J.B.; Wu, H. Atom connectivity and spectral assignments from the  $^{29}\text{Si}$ - $^{29}\text{Si}$  INADEQUATE experiment on a nanometer scale dendritic polysilane. *Magn. Res. Chem.* **2000**, *38*, 388–389.
30. Sekiguchi, A.; Lee, V.Y.; Nanjo, M. Lithiosilanes and their application to the synthesis of polysilane dendrimers. *Coord. Chem. Rev.* **2000**, *210*, 11–45.
31. Chtchian, S.; Kempe, R.; Krempner, C. Synthesis, structure and spectroscopic properties of branched oligosilanes. *J. Organomet. Chem.* **2000**, *613*, 208–219.
32. Chtchian, S.; Krempner, C. Synthesis and functionalization of branched oligosilanes. In *Organosilicon Chemistry IV: From Molecules to Materials*, 4th ed.; Auner, N., Weis, J., Eds.; Wiley-VCH Verlag GmbH: Weinheim, Germany, 2000; pp. 352–355.
33. Watanabe, A.; Nanjo, M.; Sunaga, T.; Sekiguchi, A. Dynamic of excited state of polysilane dendrimers: Origin of the broad visible emission of branched silicon chains. *J. Phys. Chem. A* **2001**, *105*, 6436–6442.
34. Oh, H.-S.; Omote, M.; Suzuki, K.; Imae, I.; Kawakami, Y. Study on the synthesis of optically active polysilane dendrimer. *Polymer Preprints* **2001**, *42*, 194–195.
35. Lambert, J.B.; Pflug, J.L.; Wu, H.; Liu, X. Dendritic polysilanes, *J. Organomet. Chem.* **2003**, *685*, 113–121.
36. Watanabe, A. Optical properties of polysilanes with various silicon skeletons. *J. Organomet. Chem.* **2003**, *685*, 122–133.
37. Krempner, C.; Reinke, H. Structure and UV spectroscopic properties of a novel dendritic oligosilane. *J. Organomet. Chem.* **2003**, *685*, 134–137.
38. Krempner, C.; Reinke, H. Synthesis and reactivity of a novel oligosilyl anion. *J. Organomet. Chem.* **2003**, *686*, 158–163.
39. Reinke, H.; Krempner, C. Synthesis and reactivity of novel oligosilyl anions. In *Organosilicon Chemistry V: From Molecules to Materials*, 5th ed.; Auner, N., Weis, J., Eds.; Wiley-VCH Verlag GmbH: Weinheim, Germany, 2003; pp. 217–222.
40. Krempner, C.; Chtchian, S.; Reinke, H. First synthesis of a dihydrido functionalized double-cored oligosilane dendrimer. *Inorg. Chim. Acta* **2004**, *357*, 3733–3738.
41. Fischer, R.; Baumgartner, J.; Kickelbick, G.; Hassler, K.; Marschner, C. Adamantanes, nortricyclenes, and dendrimers with extended silicon backbones. *Chem. Eur. J.* **2004**, *10*, 1021–1030.
42. Krempner, C.; Jäger-Fiedler, U.; Köckerling, M.; Ludwig, R.; Wulf, A. Hydroxyl substituted oligosilane dendrimers – controlling the electronic properties through hydrogen bonding. *Angew. Chem. Int. Ed.* **2006**, *45*, 6755–6759.
43. Krempner, C.; Reinke, H. The unusual absorption behavior of chloro functionalized oligosilane dendrimers. *Inorg. Chem. Commun.* **2006**, *9*, 259–262.
44. Krempner, C.; Köckerling, M.; Mamat, C. Novel double cored oligosilane dendrimers—Conformational dependence of the UV absorption spectra. *Chem. Commun.* **2006**, 720–722.

45. Krempner, C.; Reinke, H. An approach to dendritic oligosilanes – controlling the conformation through ring formation. *Organometallics* **2007**, *26*, 2053–2057.
46. Mu, T.; Feng, D.; Feng, S. A molecular modeling study of generation-dependent stability of dendritic polysilanes, *J. Theoret. Comput. Chem.* **2008**, *7*, 923–931.
47. Krempner, C.; Koeckerling, M. Nanoscale double-core oligosilane dendrimers: Synthesis, structure, and electronic properties. *Organometallics* **2008**, *27*, 346–352.
48. Krempner, C.; Jäger-Fiedler, U.; Reinke, H.; Koeckerling, M. Synthesis and structure of titanium and zirconium trisiloxides. *Organometallics* **2009**, *28*, 382–385.
49. Nanjo, M.; Sekiguchi, A. Polysilane dendrimers. In *Silicon-Containing Dendritic Polymers*; Dvornic, P., Owen, M.J., Eds.; Springer Science + Business Media B.V.: Dordrecht, The Netherlands, 2009; Volume 2, pp. 75–96.
50. Jaeger-Fiedler, U.; Koeckerling, M.; Reinke, H.; Krempner, C. Discrete oxygen containing oligosilane dendrimers: Modelling oxygen defects in silicon nanomaterials. *Chem. Comm.* **2010**, *46*, 4535–4537.
51. Gilman, H.; Smith, C.L. Tetrakis(trimethylsilyl)silane. *J. Am. Chem. Soc.* **1964**, *86*, 1454.
52. Gilman, H.; Smith, C.L. Tetrakis(trimethylsilyl)silane. *J. Organomet. Chem.* **1967**, *8*, 245–253.
53. Gilman, H.; Holmes, J.M.; Smith, C.L. Branched-chain methylated polysilanes containing a silyl-lithium group. *Chem. Ind. (Lond. UK)* **1965**, 848–849.
54. Lickiss, P.D.; Smith, C. Silicon derivatives of the metals of Groups 1 and 2. *Coord. Chem. Rev.* **1995**, *145*, 75–124.
55. Tamao, K.; Kawachi, A. Silyl anions. *Adv. Organomet. Chem.* **1995**, *38*, 1–58.
56. Wiberg, N. Sterically overloaded supersilylated main group elements and main group element clusters. *Coord. Chem. Rev.* **1997**, *163*, 217–252.
57. Belzner, J.; Dehnert, U. Alkali and Alkaline Earth Silyl Compounds-Preparation and Structure. In *The Chemistry of Organic Silicon Compounds*; Rappoport, Z., Apeloig, Y., Eds.; Wiley: Chichester, UK, 1998; Volume 2, pp.779–825.
58. Marschner, C. Preparation and reactions of polysilanyl anions and dianions. *Organometallics* **2006**, *25*, 2110–2125.
59. Kiyomori, A.; Kubota, T.; Kaneo, T.; Hasegawa, K.; Watanabe, T. Method for producing tetrakis(trimethylsilyl)silane and tris(trimethylsilyl)silane. *Jpn. Kokai Tokkyo Koho* **2001**, JP 2001192387 A.
60. Marsmann, H.C.; Raml, W.; Hengge, E. Silicon-29 nuclear resonance measurements on polysilanes. 2. Isotetrasilanes. *Z. Naturforsch. B* **1980**, *35B*, 1541–1547.
61. Notheis, C.; Brendler, E.; Thomas, B. NMR spectroscopic investigations on methylphenyl-substituted tri- and tetrasilanes. *GIT Labor-Fachzeitschrift* **1997**, *41*, 824–826.
62. Sakurai, H.; Watanabe, T.; Kumada, M. Aluminum chloride-catalyzed reactions of organosilicon compounds. IV. Preparation of tetrakis(chlorodimethylsilyl)silane and -methane. *J. Organomet. Chem.* **1967**, *9*, P11–P12.
63. Ishikawa, M.; Kumada, M.; Sakurai, H. Preparation of some polysilicon halides by aluminum halide catalyzed interchange of methyl and halogen on silicon. *J. Organomet. Chem.* **1970**, *23*, 63–69.

64. Hassler, K. Preparation of functional polysilanes: Tris(chlorodimethylsilyl)methylsilane. *Monatsh. Chem.* **1986**, *117*, 613–615.
65. Kollegger, G.; Hassler, K. Synthesis and properties of functional polysilanes: the tetrasilanes  $\text{MeSi}(\text{SiMe}_2\text{X})_3$  and hexasilanes  $(\text{Me}_2\text{XSi})_2\text{MeSiSiMe}(\text{SiMe}_2\text{X})_2$ , X = Me, H, F, Cl, Br, I. *J. Organomet. Chem.* **1995**, *485*, 233–236.
66. Herzog, U.; Schulze, N.; Trommer, K.; Roewer, G. Reaction of the Si-Cl bond with trialkyl orthoformates. Preparation of alkoxy-substituted silanes. *J. Organomet. Chem.* **1997**, *547*, 133–139.
67. Notheis, C.; Brendler, E.; Thomas, B. Chlorination of Methylphenylogosilanes: Products and reactions. In *Organosilicon Chemistry III: From Molecules to Materials*, 3rd ed.; Auner, N., Weis, J., Eds.; Wiley-VCH Verlag GmbH: Weinheim, Germany, 1998; pp. 307–311.
68. Lehnert, R.; Hoepfner, M.; Kelling, H. Silicon-29 NMR investigations on methylchlorodisilanes. *Z. Anorg. Allg. Chem.* **1990**, *591*, 209–213.
69. Herzog, U.; Richter, R.; Brendler, E.; Roewer, G. Methylchlorooligosilanes as products of the base catalyzed disproportionation of various methylchlorodisilanes. *J. Organomet. Chem.* **1996**, *507*, 221–228.
70. Gilman, H.; Smith, C.L. Tris(trimethylsilyl)silyllithium. *J. Organomet. Chem.* **1968**, *14*, 91–101.
71. Gutekunst, G.; Brook, A.G. Tris(trimethylsilyl)silyllithium 3 THF: A stable crystalline silyllithium reagent. *J. Organomet. Chem.* **1982**, *225*, 1–3.
72. Baines, K.M.; Brook, A.G.; Ford, R.R.; Lickiss, P.D.; Saxena, A.X.; Sawyer, W.J.; Behnam, B.A. Photochemical rearrangements of stable silenes. *Organometallics* **1989**, *8*, 693–709.
73. Whittaker, S.M.; Brun, M.-C.; Cervantes-Lee, F.; Pannell, K.H. Synthesis, structure, and reactivity of the permethylated decasilane  $(\text{Me}_3\text{Si})_3\text{SiSiMe}_2\text{SiMe}_2\text{Si}(\text{SiMe}_3)_3$ . *J. Organomet. Chem.* **1995**, *499*, 247–252.
74. Apeloig, Y.; Korogodsky, G.; Bravo-Zhivotovskii, D.; Blaser, D.; Boese, R. The syntheses and molecular structure of a branched oligosilyl anion with a record of nine silicon atoms and of the first branched oligosilyl dianion. *Eur. J. Inorg. Chem.* **2000**, 1091–1095.
75. Marschner, C. A new and easy route to polysilyl potassium compounds. *Eur. J. Inorg. Chem.* **1998**, 221–226.
76. Kayser, C.; Fischer, R.; Baumgartner, J.; Marschner, C. Tailor-made oligosilyl potassium compounds. *Organometallics* **2002**, *21*, 1023–1030.
77. Kayser, C.; Kickelbick, G.; Marschner, C. Simple synthesis of oligosilyl- $\alpha,\omega$ -dipotassium compounds. *Angew. Chem. (Int. Ed. Engl.)* **2002**, *41*, 989–992.
78. Mechtler, C.; Marschner, C. Polysilyldianions: Synthesis and reactivity. *Tetrahedron Lett.* **1999**, *40*, 7777–7778.
79. Note that in relatively unstrained linear and branched oligosilanes the Si-Si distances range from 234 to 236 pm and the Si-Si-Si angles deviate usually only by 3 to 4° from the ideal tetrahedral angle.
80. Stanislawski, D.A.; West, R. Silicon-29 and carbon-13 NMR spectra of permethylpolysilanes. *J. Organomet. Chem.* **1980**, *204*, 295–305.
81. Ishikawa, M.; Iyoda, J.; Ikeda, H.; Kotake, K.; Hashimoto, T.; Kumada, M. Aluminum chloride catalyzed skeletal rearrangement of permethylated acyclic polysilanes. *J. Am. Chem. Soc.* **1981**, *103*, 4845–4850.

82. Dzambaski, A.; Baumgartner, J.; Flock, M.; Hassler, K. Conformation control of oligosilanes by trimethylsilyl groups: dodecamethyl-, undecamethyl-2-trimethylsilyl- and decamethyl-2, 4-bis(trimethylsilyl)-n-pentasilane studied by Raman spectroscopy and quantum chemical calculations. *Silicon* **2010**, *1*, 225–237.
83. Lambert *et al.* [18] reported the tertiary silicon core ( $T^{3-9}$ ) of polysilane dendrimer **25**, to appear at -65.0 ppm in the  $^{29}\text{Si}$ -NMR (measured in  $\text{C}_6\text{D}_6$ ). Suzuki *et al.* [19], however, found the latter signal to be at -37.1 ppm (measured in  $\text{CDCl}_3$ ). Measuring **25** again in  $\text{C}_6\text{D}_6$  as solvent, we found chemical shifts for the central silicon core and also the other silicon nuclei being almost identical with those reported by Suzuki *et al.* [19].
84. During the preparation of this manuscript we noticed that the  $^{29}\text{Si}$ -NMR chemical shift of the central core silicon ( $T^{3-9}$ ) of polysilane dendrimer **26**, reported by Lambert and coworkers [24] to be at -66.1 ppm, did not match the expected chemical shift range for a tertiary silicon nucleus that has 3 silicon nuclei in  $\beta$ -position and 9 silicon nuclei in  $\gamma$ -position ( $T^{3-9}$ ). Note that the central  $T^{3-9}$  silicon nuclei of **25** and **56** appear at -37.1 ppm and -35.3 ppm, respectively. We independently prepared **26** by treating 3.5 equivalents of  $\text{K-Si}(\text{SiMe}_3)_2\text{SiMe}_2\text{SiMe}_2\text{Si}(\text{SiMe}_3)_3$  with one equivalent of  $\text{MeSi}(\text{SiMe}_2\text{Cl})_3$  in hexane. After aqueous workup of the reaction mixture and re-crystallization of the residue from acetone, compound **26** was isolated as a white crystalline material in 16% yield consistent with the results reported earlier by Lambert *et al.* Compound **26** was characterized by  $^1\text{H}$ -,  $^{13}\text{C}$  and  $^{29}\text{Si}$ -NMR spectroscopy. However,  $^{29}\text{Si}$ -NMR spectroscopic measurement in  $\text{CDCl}_3$  revealed the chemical shift of the central core silicon ( $T^{3-9}$ ) to be at -30.3 ppm. Although we have carried out several  $^{29}\text{Si}$ -NMR experiments, including INEPT and DEPT pulse sequences, we could not find any signal at around -66 ppm as reported by Lambert and coworkers.
85. Hsiao, Z.-L.; Waymouth, R.M. Free-radical hydrosilylation of poly(phenylsilane): Synthesis of functional polysilanes. *J. Am. Chem. Soc.* **1994**, *116*, 9779–9780.
86. Koe, J.; Powell, D.R.; Buffy, J.J.; Hayase, S.; West, R. Perchloropolysilane: X-ray structure, solid-state  $^{29}\text{Si}$  NMR spectroscopy, and reactions of  $[\text{SiCl}_2]_n$ . *Angew. Chem. Int. Ed.* **1998**, *37*, 1441–1442.
87. Herzog, U.; West, R. Heterosubstituted polysilanes. *Macromolecules* **1999**, *32*, 2210–2214.
88. Koe, J.; Motanaga, M.; Fujiki, M.; West, R. Synthesis and spectroscopic characterization of heteroatom polysilylenes: Poly(dialkoxysilylene)s and evidence for silicon  $\sigma$ -oxygen  $n$  mixing interaction. *Macromolecules* **2001**, *34*, 706–712.
89. Koe, J.R.; Fujiki, M. Heteroatom polysilylenes. *Silicon Chem.* **2002**, *1*, 77–87.
90. Obata, K.; Kira, M. Synthesis, structure, and spectroscopic properties of perhexyloligosilanes. *Organometallics* **1999**, *18*, 2216–2222.
91. Boberski, W.G.; Allred, A.L. Preparation of permethyloctadecasilane and permethyltetracosasilane. *J. Organomet. Chem.* **1974**, *71*, C27–C28.
92. Boberski, W.G.; Allred, A.L. Properties of long-chain permethylpolysilanes. *J. Organomet. Chem.* **1975**, *88*, 65–72.
93. Maxka, J.; Huang, L.M.; West, R. Synthesis and NMR spectroscopy of permethylpolysilane oligomers  $\text{Me}(\text{SiMe}_2)_{10}\text{Me}$ ,  $\text{Me}(\text{SiMe}_2)_{16}\text{Me}$ , and  $\text{Me}(\text{Me}_2\text{Si})_{22}\text{Me}$ . *Organometallics* **1991**, *10*, 656–659.

94. Michl, J.; West, R. Conformations of linear chains. Systematics and suggestions for nomenclature. *Acc. Chem. Res.* **2000**, *33*, 821–823.
95. West, R. A new theory for rotational isomeric states: polysilanes lead the way. *J. Organomet. Chem.* **2003**, *685*, 6–8.
96. Teramae, H.; Michl, J. Electronic states of linear tetrasilane and polysilanes. *Mol. Cryst. Liq. Cryst.* **1994**, *256*, 149–159.
97. Neumann, F.; Teramae, H.; Downing, J.W.; Michl, J. Gauche, ortho, and anti conformations of saturated  $A_4X_{10}$  chains: When will all six conformers exist? *J. Am. Chem. Soc.* **1998**, *120*, 573–582.
98. Albinsson, B.; Antic, D.; Neumann, F.; Michl, J. The conformers of  $n$ - $Si_5Me_{12}$ : A comparison of Ab initio and molecular mechanics methods. *J. Phys. Chem. A* **1999**, *103*, 2184–2196.
99. Tsuji, H.; Michl, J.; Tamao, K. Recent experimental and theoretical aspects of the conformational dependence of UV absorption of short chain peralkylated oligosilanes. *J. Organomet. Chem.* **2003**, *685*, 9–14.
100. Mazieres, S.; Raymond, M.K.; Raabe, G.; Prodi, A.; Michl, J. [2]Staffane rod as a molecular rack for unravelling conformer properties: Proposed singlet excitation localization isomerism in *anti,anti,anti*-Hexasilanes. *J. Am. Chem. Soc.* **1997**, *119*, 6682–6683.
101. Tamao, K.; Tsuji, H.; Terada, M.; Asahara, M.; Yamaguchi, S.; Toshimitsu, A. Conformation control of oligosilanes based on configurationally constrained bicyclic disilane units. *Angew. Chem. Int. Ed.* **2000**, *39*, 3287–3290.
102. Tsuji, H.; Terada, M.; Toshimitsu, A.; Tamao, K.  $\sigma$ - $\sigma^*$  Transition in *anti,cisoid* alternating oligosilanes: Clear-cut evidence for suppression of conjugation effect by a *cisoid* turn. *J. Am. Chem. Soc.* **2003**, *125*, 7486–7487.
103. Fukazawa, A.; Tsuji, H.; Tamao, K. All-*anti*-octasilane: Conformation control of silicon chains using the robust bicyclic trisilane as the building block. *J. Am. Chem. Soc.* **2006**, *128*, 6800–6801.
104. Tsuji, H.; Fukazawa, A.; Yamaguchi, S.; Toshimitsu, A.; Tamao, K. All-*anti* pentasilane: Conformation control of oligosilanes based on bis(tetramethylene)-tethered trisilane unit. *Organometallics* **2004**, *23*, 3375–3377.
105. Casher, D.L.; Tsuji, H.; Sano, A.; Katkevics, M.; Toshimitsu, A.; Tamao, K.; Kubota, M.; Kobayashi, T.; Ottosson, C.H.; David, D.E.; *et al.* The disilane chromophore: Photoelectron and electronic spectra of hexaalkyldisilanes and 1,( $n+2$ )-Disila[ $n.n.n$ ]propellanes. *J. Phys. Chem. A* **2003**, *107*, 3559–3566.
106. Sakamoto, K.; Naruoka, T.; Kira, M. Regulation of main-chain conformation of permethyldeasilane by complexation with  $\gamma$ -cyclodextrin. *Chem. Lett.* **2003**, *32*, 380–381.
107. Lambert, J.B.; Pflug, J.L.; Allgeier, A.M.; Campbell, D.J.; Higgins, T.B.; Singewald, E.T.; Stern, C.L. A branched polysilane. *Acta Cryst. C* **1995**, *C51*, 713–715.
108. Baumgartner, J.; Frank, D.; Kayser, C.; Marschner, C. comparative study of structural aspects of branched oligosilanes. *Organometallics* **2005**, *24*, 750–761.
109. Wallner, A.; Wagner, H.; Baumgartner, J.; Marschner, C.; Rohm, H.W.; Koeckerling, M.; Krempner, C. Structure, conformation, and UV absorption behavior of partially trimethylsilylated oligosilane chains. *Organometallics* **2008**, *27*, 5221–5229.

110. Krempner, C.; Flemming, A.; Koeckerling, M.; Ludwig, R.; Miethchen, R. Twisted oxygen containing oligosilanes: Unprecedented examples of  $\sigma$ - $n$  mixed conjugated systems. *Chem. Comm.* **2007**, 1810–1812.
111. Krempner, C.; Kopf, J.; Mamat, K.; Reinke, H.; Spannenberg, A. Novel polysilanoles via selective functionalization on oligosilanes. *Angew. Chem. (Int. Ed. Engl.)* **2004**, *43*, 5406–5408.
112. Stueger, H.; Albering, J.; Flock, M.; Fuerpass, G.; Mitterfellner, T. cis,cis-1,3,5-trihydroxynonamethylcyclohexasilane: A cyclopolysilane with unusual properties. *Organometallics* **2011**, *30*, 2531–2538.
113. Stueger, H.; Fuerpass, G.; Baumgartner, J.; Mitterfellner, T.; Flock, M. Molecular structure and UV absorption spectra of OH and NH<sub>2</sub> derivatives of dodecamethylcyclohexasilane: A combined experimental and computational study. *Z. Naturforsch. B* **2009**, *64*, 1598–1606.
114. Stueger, H.; Fuerpass, G.; Renger, K.; Baumgartner, J. Synthesis, structures, and unusual photoluminescence of O- and N-functional cyclohexasilanes. *Organometallics* **2005**, *24*, 6374–6381.
115. Renger, K.; Kleewein, A.; Stueger, H. Fluorescence of siloxy substituted cyclohexasilanes. *Phosphorus Sulfur Silicon*. **2001**, *169*, 449–452.
116. Takeda, K.; Shiraishi, K. Electronic structure of silicon-oxygen high polymers. *Solid State Commun.* **1993**, *85*, 301–305.
117. Pitt, C.G. Ultraviolet absorption spectra of derivatives of polysilanes. A probe of (p→d)<sub>π</sub> bonding in organosilicon compounds. *J. Am. Chem. Soc.* **1969**, *91*, 6613–6622.
118. Brus, L. Luminescence of silicon materials: Chains, sheets, nanocrystals, nanowires, microcrystals, and porous silicon. *J. Phys. Chem.* **1994**, *98*, 3575–3581.

© 2012 by the authors; licensee MDPI, Basel, Switzerland. This article is an open access article distributed under the terms and conditions of the Creative Commons Attribution license (<http://creativecommons.org/licenses/by/3.0/>).